

Figure 3. Induction of CD4/CD8 DP monocytes in nontransgenic rats. (A) Myocarditis was induced in FW-wt rats by immunization with porcine cardiac myosin and the adjuvant containing killed tuberculosis germs at 3 weeks of age (immunized FW-wt). Peripheral blood was obtained from the FW-wt rats one week after immunization and age-matched controls and then PBMCs in region 1 (R1) were gated as in Figure 1. In both types of rats, the majority of CD4^{medium} cells did not express CD3, thus they were considered to be monocytes. In each group, at least 3 rats were examined. Representative data are shown. (B) The expression of CD8 on peripheral monocytes (practically CD4^{medium} cells) was examined 1 week and 4 weeks after immunization (4 and 7 weeks of age, respectively). Data were compared with those of nonimmunized FW-wt (control FW-wt) and FW-pX rats. In each group, at least 3 rats were examined. Representative data are shown. (C) The percentage of CD8⁺ cells in monocytes 1 week and 4 weeks after immunization (4 and 7 weeks of age, respectively) is shown as mean \pm SD. (D) Inbred F344 rats (3 weeks of age) were immunized with various combinations of components used for the induction of myosin-induced myocarditis. The percentage of CD8⁺ cells in monocytes was examined 1 week after immunization. In each experiment, at least 3 rats were used. Data are represented as mean \pm SD. FIA indicates Freund incomplete adjuvant; Killed G, killed tuberculosis germs. (E) PBMCs from F344 rats (3 weeks old) were incubated with IL-12, RANTES, or GM-CSF under indicated concentrations. We chose these cytokines because they are known to be induced by BCG.³¹⁻³³ Twenty-four hours later, the percentage of CD8⁺ cells in monocytes (practically CD4^{medium} cells) was examined. Data are represented as mean \pm SD of repeated experiments done in triplicate. **P* < .05.

findings indicate that DP monocytes can be induced in rats without any influence of the *pX* transgene and suggest that they may be induced in an acute inflammatory phase.

To investigate the induction mechanisms of DP monocytes, we next immunized inbred F344 rats with various combinations of individual components used for initial immunization. When rats were immunized with the adjuvant containing killed tuberculosis germs, the percentage of CD8⁺ population in CD4^{medium} cells was increased in the largest scale, though significant differences were observed by addition of any of the components (incomplete adjuvant only, an increase of 7.7%; adjuvant plus killed tuberculosis germs, an increase of 21.4%; myosin plus adjuvant plus killed tuberculosis germs, an increase of 29.9%; Figure 3D). This suggested that immunization with tuberculosis germs might be critical for the induction of DP monocytes. To test this hypothesis, we examined whether the cytokines and chemokines known to be induced by the recombinant *Mycobacterium bovis* bacillus Calmette-Guerin

(BCG)³²⁻³⁴ can induce DP monocytes in vitro. PBMCs from F344 rats were stimulated with IL-12, RANTES, or GM-CSF for 24 hours and then the percentage of DP monocytes was measured. Among these cytokines/chemokines, only GM-CSF could induce DP monocytes in a dose-dependent manner (Figure 3E). We also observed that the percentage of DP monocytes (CD4^{medium} CD8⁺ population in PBMCs) was increased from 7.8% to 11.0% by in vivo administration of GM-CSF. However, stimulation of bone marrow cells by GM-CSF failed to induce any significant expansion of CD4⁺/CD8⁺ cells (data not shown).

Infiltration of CD4⁺/CD8⁺ cells at the site of myocarditis

In myosin-immunized FW-wt rats, myocarditis occurred 3 to 4 weeks after immunization (Figure 4A). At the site of inflammation, macrophages (reactive with ED-1, Figure 4B) infiltrated more abundantly than CD3⁺ T cells (Figure 4C). To determine if

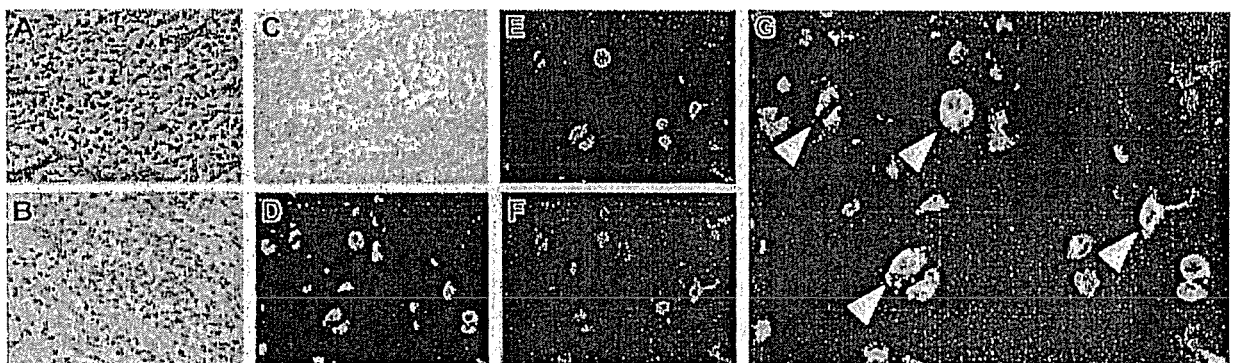


Figure 4. Infiltration of DP macrophages at the site of myocarditis. Myocarditis was induced in FW-wt rats by immunization with porcine myosin and the adjuvant containing killed tuberculosis germs at 3 weeks of age. Three weeks later, the heart was extirpated and used for histologic and immunocytochemical examinations. Experiments were repeated twice. Representative results are shown. (A) Hematoxylin and eosin staining. (B-C) Immunohistochemical staining for CD68 (ED-1) and CD3 (IF4), respectively. The cardiac tissues were cut into small pieces and digested with 0.16% collagenase type II. After removal of tissue fragments, cell suspension was incubated in a plastic dish at 37°C. One hour later, adherent cells were harvested and immunofluorescent triple staining was done for CD68 (ED-1, green; D), CD4 (OX-35, red; E), and CD8 (OX-8, blue; F). (G) The merged image. Arrowheads indicate DP macrophages also stained for CD68. Total magnification: \times 40 (A-C), \times 80 (D-F), and \times 200 (G).

infiltrating cells contained DP macrophages, adherent cells were isolated from collagenase-digested cardiac tissues and subjected to immunocytochemical analysis. Half of macrophages (reactive with ED-1) expressed both CD4 and CD8 (Figure 4D-G). These DP macrophages were not reactive with ED-2 (a marker for tissue-resident macrophages²⁵) or OX-62 (a marker for DCs; data not shown). Thus, infiltrating DP macrophages are neither tissue-resident macrophages nor DCs but are derived from the blood.

Cytokine/chemokine profiles and the cytotoxic phenotype of CD4/CD8 DP macrophages

We isolated adherent cells from rat cardiac tissues affected with myocarditis and separated DP macrophages from other, practically CD8⁻ macrophages (hereafter referred to as CD8⁻ macrophages) using the MACS system (Figure 5A). We then compared expression profiles of cytokines, chemokines, and cytotoxic factors by quantitative real-time RT-PCR in DP and CD8⁻ macrophages. DP macrophages showed higher expression of IL-18 (5.2-fold), IFN- γ (2.8-fold), and RANTES (4.8-fold) in comparison with CD8⁻ macrophages (Figure 5B). By contrast, the expression of MCP-1 was lower in DP macrophages than in CD8⁻ macrophages (1/4.7-fold). There was no significant difference in the expression of IL-4, IL-12, monocyte-derived chemokine (MDC), or TGF- β , or TNF- α between DP and CD8⁻ macrophages (data not shown). When we focused on cytotoxic factors, DP macrophages showed significantly higher expression of Fas L (8.0-fold), perforin (9.2-fold), and granzyme B (45.9-fold) compared with CD8⁻ macrophages (Figure 5C). Expression of iNOS did not show a significant difference between DP and CD8⁻ macrophages (data not shown). When we examined the expression of Fas L and granzyme B in tissue-infiltrating macrophages by immunohistochemistry, colocalization of these molecules and ED-1 (CD68) was observed (Figure 5D left panels). To rule out the possibility that ED-1-positive (CD68⁺) cells are overlaid with scattered, secreted granzyme B, we examined the expression of granzyme B in macrophages isolated from the cardiac tissue (Figure 5D right panel). These experiments confirmed that part of ED-1-positive (CD68⁺) macrophages did express Fas L and granzyme B.

DP monocytes are precursors of DP macrophages

To determine if DP monocytes in the blood migrated into sites of inflammation and differentiated to DP macrophages, transfer of GFP-positive spleen cells was made into nontransgenic rats immunized with myosin. GFP-positive macrophages were found in cardiac tissues with myocarditis (Figure 6A), and some GFP-positive macrophages expressed both CD4 and CD8 (Figure 6B). Furthermore, when the profiles of DP monocytes and DP macrophages were compared by RT-PCR, the expression patterns of Fas L, perforin, and granzyme B were similar (Figure 6C). On the other hand, the expression of NKR-P2 (rat orthologue of human NKG2D³⁵), known to play an important role in killing by NK cells and cytotoxic T lymphocytes (CTLs),^{36,37} was higher only in DP macrophages. These findings suggest that DP monocytes are precursors of tissue-infiltrating DP macrophages with a cytotoxic phenotype. In our experiments, evaluation of contaminated CD8⁺ CTLs was critical. As previously described, the purity of macrophages in the cells recovered from the cardiac tissues with myocarditis was 94% (see "Isolation of macrophages from cardiac tissues, with myocarditis"). We therefore used a mixed cDNA sample (a mixture of CD8⁺ T cells and fibroblasts in a ratio

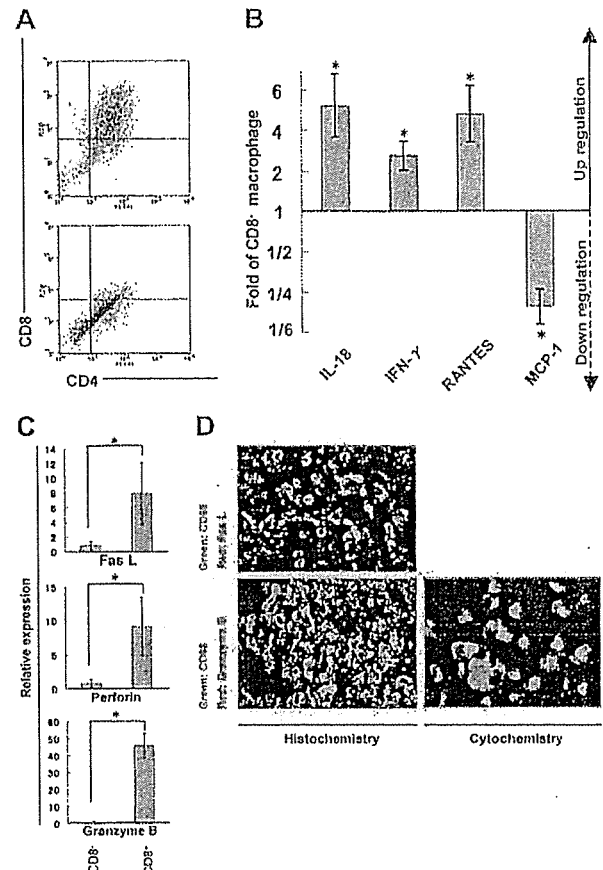


Figure 5. Expression profiles of cytokines/chemokines and cytotoxic factors in DP macrophages. Infiltrating macrophages were isolated from the cardiac tissues by collagenase digestion followed by adhesion to the plastic dish. DP macrophages were separated from other macrophages by MACS based on the presence or absence of CD8. Prior to the MACS sorting, we confirmed by light microscopy that macrophages detached from the plastic dish were in a single-cell suspension (data not shown). (A) Macrophages collected from the cardiac tissues were reacted with FITC-conjugated anti-CD4 (OX-35) and PE-conjugated anti-CD8 (OX-8) Abs. MACS was conducted using anti-PE microbeads. The cells selected positively and negatively are shown in the top and bottom panels, respectively. Experiments were repeated at least twice, and representative results are shown. (B) The expression of cytokines/chemokines (IL-18, IFN- γ , RANTES, and MCP-1) in DP macrophages was analyzed by quantitative real-time RT-PCR. The data were compared with those of CD8⁻ macrophages. Results are represented as a fold (mean \pm SD of repeated experiments done in triplicate) against control macrophages. (C) The expression patterns of cytotoxic factors (Fas L, perforin, and granzyme B) in DP macrophages (right columns) were compared with those in CD8⁻ macrophages (left columns). Data are represented as mean \pm SD of repeated experiments done in triplicate. (D) Immunofluorescent double staining for CD68 (ED-1, green) and Fas L (N-20, red), or CD68 (ED-1, green) and granzyme B (N-19, red) in the cardiac tissue section (left panels). Infiltrating macrophages isolated from the tissues were stained for CD68 (ED-1, green) and granzyme B (N-19, red; right panel). Total magnification: \times 80. * $P < .05$.

of 1:9) as a negative control. In this negative control, the expression of CD3, NKR-P2, Fas L, perforin, and granzyme B was hardly detectable, whereas the expression level of the *Gapdh* gene was comparable to that of other samples. Although these experiments do not provide information as to the identity of CD4⁺/CD8⁺ DP cells or assure the absence of contamination of T cells in the samples, they indicate that NKR-P2, Fas L, perforin, and granzyme B are produced by DP monocytes/macrophages. Moreover, immunocytochemistry demonstrated the existence of granzyme B-containing granules in CD8⁺ CD68⁺ adherent splenocytes regarded as DP monocytes (Figure 6D).

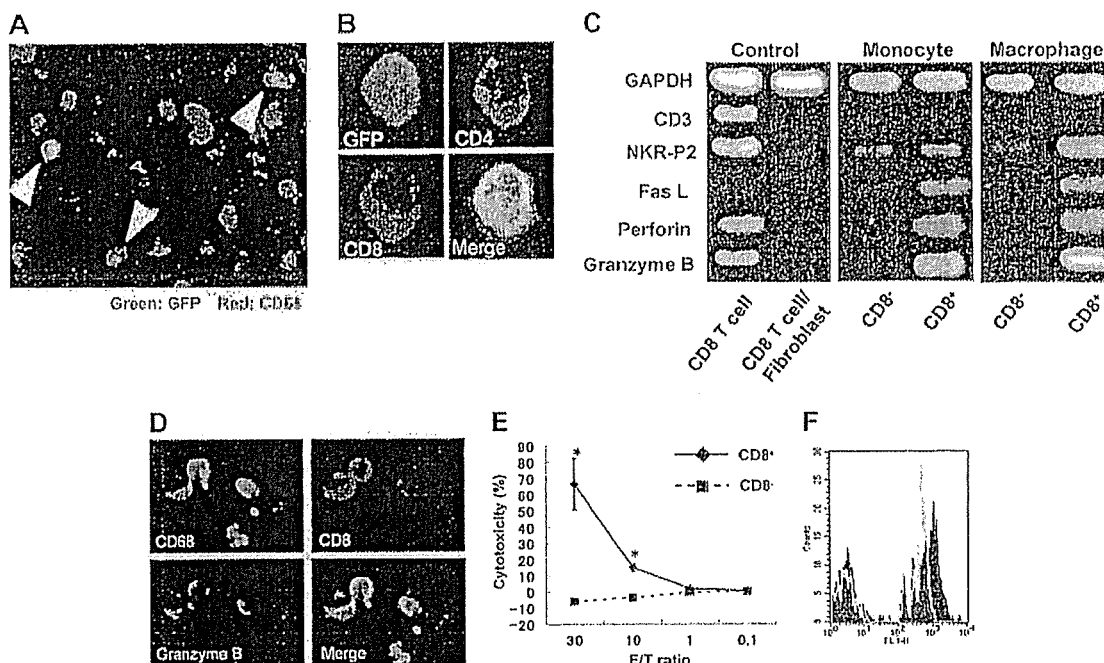


Figure 6. Origin of CD4/CD8 DP macrophages and function of CD4/CD8 DP monocytes. (A) GFP-positive spleen cells were transferred into GFP-negative recipients that had been immunized with porcine myosin. EGFP transgenic rats and nontransgenic Wistar rats (all rats were 4 weeks old) were immunized with myosin as described in "Immunization of rats with porcine heart myosin and induction of myocarditis." Mononuclear cells were isolated from the spleen of EGFP transgenic rats 1 week after immunization and transferred into Wistar rats intravenously 2 weeks after immunization (1×10^7 cells per animal). Five days later, the hearts of recipients were extirpated, and then tissue-infiltrating macrophages were isolated and used. Experiments were repeated twice, and representative results are shown. Arrowheads indicate cells expressing both GFP and CD68 (ED-1, red). Total magnification: $\times 100$. (B) The cells isolated from the cardiac tissues were cultured in chamber slides at 37°C for 1 hour. Resultant adherent cells were fixed using cold acetone for 5 minutes and then stained for CD4 (OX-35, red) and CD8 (OX-8, blue). The merged image shows that the cell expressing both CD4 and CD8 is also positive for GFP. Total magnification: $\times 600$. (C) FW-wt rats were immunized with myosin and the adjuvant containing killed tuberculosis germs. Mononuclear cells separated from the spleen or cardiac tissues 1 week or 3 weeks after immunization, respectively, were cultured in plastic dishes at 37°C for 1 hour, and then the adherent cells were divided into CD8⁻ and CD8⁺ populations, using the MACS system. Expression profiles of CD3, NKR-P2, Fas L, perforin, and granzyme B were compared by RT-PCR. The cDNA from CD8⁺ T cells served as a positive control. The negative control was the cDNA derived from the 1:9 mixture of CD8⁺ T cells and fibroblasts. (D) Six-week-old Wistar rats were immunized with adjuvants containing killed tuberculosis germs. One week later, mononuclear cells were separated from the spleen and then cultured in chamber slides at 37°C for 1 hour. Resultant adherent cells were fixed using cold acetone for 5 minutes, followed by staining for CD68 (ED-1, green), granzyme B (red), and CD8 (OX-8, blue). The merged image shows the cells stained with 3 colors. Total magnification: $\times 200$. (E) Cytotoxic assay in vitro. Six-week-old Wistar rats were immunized with adjuvants containing killed tuberculosis germs. One week later, mononuclear cells were separated from the spleen and incubated in plastic dishes for 20 minutes at 37°C . Resultant adherent cells were collected and divided into CD8⁻ and CD8⁺ cells using the MACS system. These cells were added to the culture of allogenic epithelial thymoma cells with E/T ratios of 30, 10, 1, and 0.1 (4×10^4 target cells per well in 24-well plates). After incubation for 18 hours, cytotoxicity was measured using the CytoTox 96 test kit. Data are represented as mean \pm SD of experiments done in triplicate. * $P < .05$. (F) Phagocytosis assay. Yellow-green carboxylate-modified 1.0 μm latex beads were mixed with peripheral blood from Wistar rats that had been immunized with adjuvants containing killed tuberculosis germs one week before (1.5×10^7 beads/300 μL blood). After incubation for 2 hours at 37°C , PE-conjugated anti-CD4 (OX-35) and PerCP-conjugated anti-CD8 (OX-8) Abs were added to the mixture, followed by depletion of erythrocytes. After 3 times wash with cold PBS, CD4⁺/CD8⁺ cells were gated to determine uptake of the fluorescence-labeled beads using FACScan. Experiments were done in triplicate. Representative results are shown. The filled and gray histograms represent the profiles of CD4⁺/CD8⁺ and CD4⁺/CD8⁻ monocytes, respectively.

Cytotoxic function of DP monocytes

In order to evaluate the function of DP monocytes, we carried out in vitro cytotoxic assays against allogenic tumor cells. As a source of DP monocytes, we used CD8⁺ adherent splenocytes obtained from Wistar rats that had been immunized with adjuvants containing killed tuberculosis germs. These cells effectively killed epithelial thymoma cells originated from F344 rats carrying the HTLV-I *pX* transgene¹⁹ in a dose-dependent manner (Figure 6E). When the E/T ratio was 30, percent specific lysis was 70.8 ± 6.8 . By contrast, CD8⁻ monocytes hardly killed the tumor cells. These findings clearly indicate that DP monocytes possess a cytotoxic function and that these cells can kill tumor cells without major histocompatibility complex (MHC) restriction.

Phagocytic ability of DP monocytes

To determine the phagocytic ability of DP monocytes, yellow-green carboxylate-modified 1.0- μm latex beads were mixed with

peripheral blood from Wistar rats that had been immunized with adjuvants containing killed tuberculosis germs one week before (1.5×10^7 beads/300 μL blood). After incubation for 2 hours at 37°C , uptake of fluorescence-labeled beads in DP monocytes was assayed using FACScan (Figure 6F). The black histogram indicates that the majority of DP monocytes ($71.1\% \pm 4.4\%$) engulfed the beads during the experimental period. Phagocytic efficiency of DP monocytes was almost equivalent to that of CD4⁺/CD8⁻ monocytes ($67.4\% \pm 8.8\%$; Figure 6F gray histogram).

DP monocytes in the human peripheral blood

To examine whether humans also have DP monocytes, we analyzed PBMCs from 12 healthy volunteers by 3-color FCM. CD4⁺/CD8⁺ cells were identified in CD14⁺ monocytes in all samples examined (Figure 7). The percentage of CD4⁺/CD8⁺ cells in CD14⁺ monocytes showed considerable individual variations ranging from 17.3% to 1.0%.

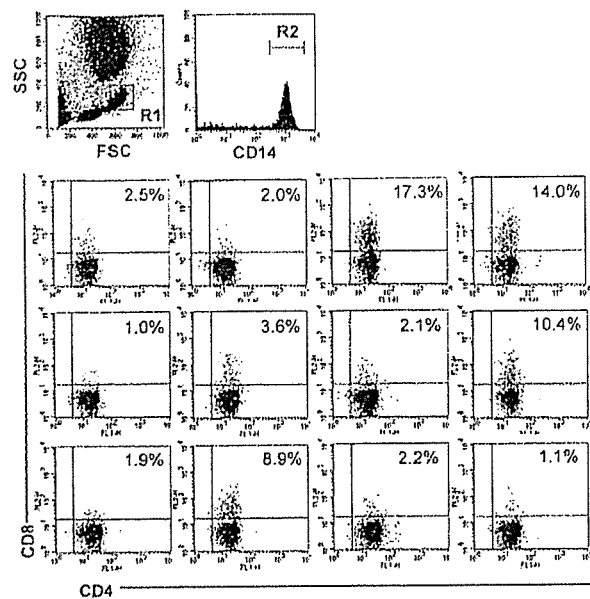


Figure 7. CD4/CD8 DP monocytes in human peripheral blood. Human peripheral blood was obtained from 12 healthy volunteers. The cells were stained with FITC-conjugated anti-CD4 (M-T466), PE-conjugated anti-CD8 (HIT8a), and PerCP-conjugated anti-CD14 (M ϕ P9) Abs, followed by depletion of erythrocytes, and then monocytes in region 1 (R1) were gated. The bottom panels show expression of CD4 and CD8 on CD14⁺ cells in region 2 (R2). The percentage of CD4⁺/CD8⁺ cells in CD14⁺ monocytes is shown in each panel.

Discussion

In the present study, we have identified a population of monocytes/macrophages characterized by coexpression of CD4 and CD8. This population was originally identified in FW-pX rats carrying the HTLV-I pX transgene (Figures 1-2) but later found to be present in wild-type rats (Figure 3). The number of DP monocytes showed a dramatic increase in rats with myosin-induced myocarditis (Figure 3), and the DP macrophages were predominant infiltrating cells at the cardiac lesion (Figure 4). The most notable feature characterizing this population of macrophages is that they express high levels of Fas L, perforin, granzyme B (Figure 5C-D), and NKR-P2 (Figure 6C). In particular, granzyme B was expressed at an extremely high level (45.9-fold) in DP macrophages compared with CD8⁻ macrophages (Figure 5C). NKG2D is the receptor previously shown to be expressed on NK cells, CTLs, and activated macrophages.³⁸ It binds to stress-inducible MHC class I molecules, MICA/B, and ULBP/RAET1 in humans and RAE-1 (retinoic acid early inducible-1) in mice.^{36,37} NK cells and CTLs bind to the target cells through NKG2D and destroy them through coordinated actions of perforin and cytotoxic factors such as granzyme B. Thus, the collective evidence clearly indicates that tissue-infiltrating DP macrophages exhibit a cytotoxic phenotype. They may therefore contribute to tissue damage by adhering to target cells via their NKR-P2 and secreting perforin and granzyme B.

Another notable feature of CD4/CD8 DP macrophages is that they express IL-18, IFN- γ , and RANTES at higher levels and MCP-1 at a lower level than CD8⁻ macrophages (Figure 5B). IL-18, IFN- γ , and RANTES induce the T-helper 1 (Th1)-type immune response,^{33,39,40} whereas MCP-1 induces the Th2-type immune response.⁴¹ Although we were unable to detect *Cd3* mRNA by RT-PCR in our macrophage samples (Figure 6C),

contamination of a small number of T/NK cells cannot be ruled out. Therefore, we should keep in mind the possibility that the cytokine production profiles (Figure 5B) may have been affected by contaminating T/NK cells; this reservation applies especially to IFN- γ , a cytokine typically produced by T/NK cells. However, we can say that tissue-infiltrating DP macrophages are prone to induce IL-18 and Th1-type immune responses at the site of inflammation. Okura et al⁴² reported that Th1 cytokines were the major cytokines detected in the early phase of myosin-induced experimental myocarditis in rats. Our present study indicates that DP macrophages infiltrating in the cardiac lesion may enhance the Th1-type immune response observed in the early phase of myosin-induced myocarditis.

The number of DP monocytes showed a dramatic increase by immunization with myosin (Figure 3B-C). When we examined which component in the immunogen was critical for increasing the population of DP monocytes, we found that the killed tuberculosis germs were the most effective factors (Figure 3D). BCG containing killed tuberculosis germs works synergistically with IL-18 for induction of IFN- γ and GM-CSF and induces the Th1-type immune response.³³ GM-CSF increased the number of DP monocytes in a dose-dependent manner in vitro (Figure 3E). These findings suggested that the secretion of GM-CSF induced by immunization with the killed tuberculosis germs triggered the expansion of DP monocytes in peripheral blood. The kinetics of expansion suggest that an increase in the number of DP monocytes occurs in the early phase of inflammation.

To examine whether CD4⁺/CD8⁺ cells are derived from DP monocytes in blood or are generated in situ from resident macrophages, we transferred GFP-positive spleen cells into GFP-negative recipients that had been immunized with myosin in advance (Figure 6A-B). This adoptive transfer experiment clearly indicates that tissue-infiltrating DP macrophages are of hematogenous origin. Consistent with this observation, DP macrophages in situ did not express ED-2 (a marker for tissue-resident macrophages) or OX-62 (a marker for DCs). Thus, overall data indicate that certain stimuli that induce the release of GM-CSF trigger the expansion of DP monocytes in peripheral blood and that these cells migrate to the site of inflammation and differentiate into macrophages displaying the Th1-type immune response and a cytotoxic phenotype. In line with these findings, DP monocytes could kill allogenic tumor cells in vitro (Figure 6E). This killing is unlikely to be mediated by the CTLs contaminated in the effector cells because CTLs can kill only MHC-matched targets. In addition, we demonstrated that DP monocytes were equipped with phagocytic activities comparable to those of CD4⁺/CD8⁻ monocytes (Figure 6F).

Interestingly, human peripheral blood also contains CD14⁺ monocytes expressing both CD4 and CD8 (Figure 7). In this regard, it is notable that DP macrophage/dendritic cells, which express Fas L more abundantly than other macrophages, have been identified in the thyroid glands of patients with autoimmune thyroid diseases.⁴³ Although the information available on their surface markers and cytokine profiles precludes us from drawing any conclusions, it is possible that they are derived from the DP monocytes identified in this study.

All volunteers who participated in this study were healthy donors. None of the donors apparently suffered from inflammatory, autoimmune, or neoplastic disorders. It is of great interest to examine whether a population of DP monocytes is increased in

blood under infectious or other disease conditions. Studies along this line are ongoing using clinical samples. Whereas rat DP monocytes displayed cytotoxicity against allogenic tumor cells (Figure 6E), we have thus far been unable to demonstrate cytotoxic activities for human DP monocytes. This may be related to the fact that human DP monocytes were isolated from healthy volunteers, whereas rat DP monocytes were isolated from animals whose immune systems were activated by the transgene or artificial immunization. Studies are in progress to understand whether the rat

and human DP monocytes/macrophages have any specialized roles in host defense against infection or cancer and in the pathogenesis of autoimmune disorders.

Acknowledgments

We thank Ken-ichi Nakase, Chisato Sudo, and Masayo Tateyama for technical assistance.

References

- Laskin DL, Weinberger B, Laskin JD. Functional heterogeneity in liver and lung macrophages. *J Leukoc Biol*. 2001;70:163-170.
- Stout RD, Suttles J. Functional plasticity of macrophages: reversible adaptation to changing microenvironments. *J Leukoc Biol*. 2004;76:509-513.
- Mantovani A, Sozzani S, Locati M, Allavena P, Sica A. Macrophage polarization: tumor-associated macrophages as a paradigm for polarized M2 mononuclear phagocytes. *Trends Immunol*. 2002;23:549-555.
- Kikuchi K, Ikeda H, Tsuchikawa T, et al. A novel animal model of thymic tumour: development of epithelial thymoma in transgenic rats carrying human T lymphocyte virus type I pX gene. *Int J Exp Pathol*. 2002;83:247-255.
- Baba T, Ishizu A, Ikeda H, et al. Chronic graft-versus-host disease-like autoimmune disorders spontaneously occurred in rats with neonatal thymus atrophy. *Eur J Immunol*. 2005;35:1731-1740.
- Jefferies WA, Green JR, Williams AF. Authentic T helper CD4 (W3/25) antigen on rat peritoneal macrophages. *J Exp Med*. 1985;162:117-127.
- Wood GS, Warner NL, Warnke RA. Anti-Leu-3/T4 antibodies react with cells of monocyte/macrophage and Langerhans lineage. *J Immunol*. 1983;131:212-216.
- Kim MS, Kim SH, Lee HJ, Kim HM. Expression and function of CD8 alpha/beta chains on rat and human mast cells. *Biol Pharm Bull*. 2004;27:399-403.
- Popovich PG, van Rooijen N, Hickey WF, Preidis G, McGaughy V. Hematogenous macrophages express CD8 and distribute to regions of lesion cavitation after spinal cord injury. *Exp Neurol*. 2003;182:275-287.
- Shortman K, Liu YJ. Mouse and human dendritic cell subtypes. *Nat Rev Immunol*. 2002;2:151-161.
- Hirji NS, Lin TJ, Gilchrist M, et al. Novel CD8 molecule on macrophages and mast cells: expression, function and signaling. *Int Arch Allergy Immunol*. 1999;118:180-182.
- Lin TJ, Hirji N, Nohara O, Stenton GR, Gilchrist M, Befus AD. Mast cells express novel CD8 molecules that selectively modulate mediator secretion. *J Immunol*. 1998;161:6265-6272.
- Hirji N, Lin TJ, Befus AD. A novel CD8 molecule expressed by alveolar and peritoneal macrophages stimulates nitric oxide production. *J Immunol*. 1997;158:1833-1840.
- Torres-Nagel N, Kraus E, Brown MH, et al. Differential thymus dependence of rat CD8 isoform expression. *Eur J Immunol*. 1992;22:2841-2848.
- Hirabayashi M, Kato M, Aoto T, et al. Offspring derived from intracytoplasmic injection of transgenic rat sperm. *Transgenic Res*. 2002;11:221-228.
- Pelidou SH, Zou LP, Deretzi G, et al. Intranasal administration of recombinant mouse interleukin-12 increases inflammation and demyelination in chronic experimental autoimmune neuritis in Lewis rats. *Scand J Immunol*. 2000;51:29-35.
- Hayase H, Ishizu A, Ikeda H, et al. Aberrant gene expression by CD25+CD4+ immunoregulatory T cells in autoimmune-prone rats carrying the human T cell leukemia virus type-I gene. *Int Immunol*. 2005;17:677-684.
- Bloch G, Toma DP, Robinson GE. Behavioral rhythmicity, age, division of labor and period expression in the honey bee brain. *J Biol Rhythms*. 2001;16:444-456.
- Tsuji T, Ikeda H, Tsuchikawa T, et al. Malignant transformation of thymoma in recipient rats by heterotopic thymus transplantation from HTLV-I transgenic rats. *Lab Invest*. 2005;85:851-861.
- Nascimbeni M, Shin EC, Chiriboga L, Kleiner DE, Rehermann B. Peripheral CD4(+)CD8(+) T cells are differentiated effector memory cells with antiviral functions. *Blood*. 2004;104:478-486.
- Robinson AP, White TM, Mason DW. Macrophage heterogeneity in the rat as delineated by two monoclonal antibodies MRC OX-41 and MRC OX-42, the latter recognizing complement receptor type 3. *Immunology*. 1986;57:239-247.
- Scriba A, Schneider M, Grau V, van der Meide PH, Steiniger B. Rat monocytes up-regulate NKR-P1A and down-modulate CD4 and CD43 during activation in vivo: monocyte subpopulations in normal and IFN-gamma-treated rats. *J Leukoc Biol*. 1997;62:741-752.
- Kraus E, Lambracht D, Wönigelt K, Hunig T. Negative regulation of rat natural killer cell activity by major histocompatibility complex class I recognition. *Eur J Immunol*. 1996;26:2582-2586.
- Brenan M, Puklavec M. The MRC OX-62 antigen: a useful marker in the purification of rat velle cells with the biochemical properties of an integrin. *J Exp Med*. 1992;175:1457-1465.
- Hines JE, Johnson SJ, Burt AD. In vivo responses of macrophages and perisinusoidal cells to cholestatic liver injury. *Am J Pathol*. 1993;142:511-518.
- Dijkstra CD, Dopp EA, Joling P, Kraal G. The heterogeneity of mononuclear phagocytes in lymphoid organs: distinct macrophage subpopulations in the rat recognized by monoclonal antibodies ED1, ED2 and ED3. *Immunology*. 1985;54:589-599.
- Hameed A, Hruban RH, Gage W, Pettis G, Fox WM 3rd. Immunohistochemical expression of CD68 antigen in human peripheral blood T cells. *Hum Pathol*. 1994;25:872-876.
- Pullford KA, Sipos A, Cordell JL, Stross WP, Mason DY. Distribution of the CD68 macrophage/myeloid associated antigen. *Int Immunol*. 1990;2:973-980.
- Filion LG, Izaguirre CA, Garber GE, Huebsh L, Aye MT. Detection of surface and cytoplasmic CD4 on blood monocytes from normal and HIV-1 infected individuals. *J Immunol Methods*. 1990;135:59-69.
- Moebius U, Kober G, Griscelli AL, Hercend T, Meuer SC. Expression of different CD8 isoforms on distinct human lymphocyte subpopulations. *Eur J Immunol*. 1991;21:1793-1800.
- Shin J, Doyle C, Yang Z, Kappes D, Strominger JL. Structural features of the cytoplasmic region of CD4 required for internalization. *EMBO J*. 1990;9:425-434.
- Higuchi K, Sekiya Y, Harada N. Characterization of M. Tuberculosis-derived IL-12-inducing material by alveolar macrophages. *Vaccine*. 2004;22:724-734.
- Luo Y, Yamada H, Chen X, et al. Recombinant Mycobacterium bovis bacillus Calmette-Guérin (BCG) expressing mouse IL-18 augments Th1 immunity and macrophage cytotoxicity. *Clin Exp Immunol*. 2004;137:24-34.
- Mendez-Samperio P, Vazquez A, Ayala H. Infection of human monocytes with Mycobacterium bovis BCG induces production of CC-chemokines. *J Infect*. 2003;47:139-147.
- Alli R, Saviliri B, Das S, Varalakshmi C, Rangaraj N, Khar A. Involvement of NKR-P2/NKG2D in DC-mediated killing of tumor targets: indicative of a common, innate, target-recognition paradigm? *Eur J Immunol*. 2004;34:1119-1126.
- Verneris MR, Karami M, Baker J, Jayaswal A, Negrin RS. Role of NKG2D signaling in the cytotoxicity of activated and expanded CD8+ T cells. *Blood*. 2004;103:3065-3072.
- Diefenbach A, Raulet DH. Strategies for target cell recognition by natural killer cells. *Immunol Rev*. 2001;181:170-184.
- Diefenbach A, Jamieson AM, Liu SD, Shastri N, Raulet DH. Ligands for the murine NKG2D receptor: expression by tumor cells and activation of NK cells and macrophages. *Nat Immunol*. 2000;1:119-126.
- Sin J, Kim JJ, Pachuk C, Satishchandran C, Weiner DB. DNA vaccines encoding interleukin-8 and RANTES enhance antigen-specific Th1-type CD4(+) T-cell-mediated protective immunity against herpes simplex virus type 2 in vivo. *J Virol*. 2000;74:11173-11180.
- Kawal T, Seki M, Hiromatsu K, et al. Selective diapedesis of Th1 cells induced by endothelial cell RANTES. *J Immunol*. 1999;163:3269-3278.
- Gu L, Tseng S, Horner RM, Tam C, Loda M, Rollins BJ. Control of TH2 polarization by the chemokine monocyte chemoattractant protein-1. *Nature*. 2000;404:407-411.
- Okura Y, Takeda K, Honda S, et al. Recombinant murine interleukin-12 facilitates induction of cardiac myosin-specific type 1 helper T cells in rats. *Circ Res*. 1998;82:1035-1042.
- Nakamura Y, Watanabe M, Matsuzuka F, Maruoka H, Mlyauchl A, Iwatani Y. Intrathyroidal CD4+ T lymphocytes express high levels of Fas and CD4+ CD8+ macrophages/dendritic cells express Fas ligand in autoimmune thyroid disease. *Thyroid*. 2004;14:819-824.

Role of Neuronal Interferon- γ in the Development of Myelopathy in Rats Infected with Human T-Cell Leukemia Virus Type 1

Yukiko Miyatake, Hitoshi Ikeda, Akihiro Ishizu, Tomohisa Baba, Toru Ichihashi, Akira Suzuki, Utano Tomaru, Masanori Kasahara, and Takashi Yoshiki

From the Department of Pathology/Pathophysiology, Division of Pathophysiological Science, Hokkaido University Graduate School of Medicine, Sapporo, Japan

Human T-cell leukemia virus type 1 (HTLV-1) is the causative agent of not only adult T-cell leukemia but also HTLV-1-associated myelopathy/tropical spastic paraparesis (HAM/TSP). Among the rat strains infected with HTLV-1, chronic progressive myelopathy, named HAM rat disease, occurs exclusively in WKAH rats. In the present study, we found that HTLV-1 infection induces interferon (IFN)- γ production in the spinal cords of HAM-resistant strains but not in those of WKAH rats. Neurons were the major cells that produced IFN- γ in HTLV-1-infected, HAM-resistant strains. Administration of IFN- γ suppressed expression of *pX*, the gene critically involved in the onset of HAM rat disease, in an HTLV-1-immortalized rat T-cell line, indicating that IFN- γ protects against the development of HAM rat disease. The inability of WKAH spinal cord neurons to produce IFN- γ after infection appeared to stem from defects in signaling through the interleukin (IL)-12 receptor. Specifically, WKAH-derived spinal cord cells were unable to up-regulate the *IL-12 receptor β 2* gene in response to IL-12 stimulation. We suggest that the failure of spinal cord neurons to produce IFN- γ through the IL-12 pathway is involved in the development of HAM rat disease. (Am J Pathol 2006, 169:189–199; DOI: 10.2353/ajpath.2006.051225)

Human T-cell leukemia virus type 1 (HTLV-1) is the causative agent of adult T-cell leukemia (ATL)^{1,2} and so-called HTLV-1-associated diseases such as HTLV-1-associated myelopathy/tropical spastic paraparesis (HAM/TSP),^{3,4} HTLV-1 uveitis (HU),⁵ HTLV-1-associated arthropathy (HAAP),⁶ T-cell alveolitis,⁷ Sjögren's syndrome,⁸ polymy-

ositis,⁹ and infective dermatitis.¹⁰ Only a small proportion (<5%) of HTLV-1-infected individuals develop ATL or HTLV-1-associated diseases, whereas more than 95% of carriers remain asymptomatic for life.¹¹ Little is known about the factors that govern susceptibility to diseases caused by HTLV-1.

We previously established a rat model of HAM/TSP in which chronic progressive myelopathy with paraparesis of lower limbs occurred in WKAH rats 15 to 22 months after HTLV-1 infection.¹² Although the provirus was detected in the systemic organs of all HTLV-1-infected strains examined, myelopathy, hereafter referred to as HAM rat disease, occurred exclusively in WKAH rats. Histopathological alterations were limited to the thoracic spinal cord in HAM rat disease. The most crucial finding was apoptotic cell death of oligodendrocytes in the anterior and lateral funiculi of the upper thoracic cord, which became manifest 7 months after inoculation with HTLV-1.¹³ Subsequently, demyelination occurred with infiltration of activated macrophages, and at the end stage of the disease, proliferation of astrocytes was observed in the affected region.¹⁴ Interestingly, lymphocytic infiltration into the spinal cord, which is characteristic of human HAM/TSP,¹⁵ was absent throughout the disease process in the HAM rat model. Although the significance of this finding is not clear, lymphocytic infiltration in human HAM/TSP may represent a cellular response to tissue damage.

The HTLV-1 provirus, which predominantly localizes in microglia and macrophages, becomes detectable in the spinal cord of both HAM-resistant and -susceptible rats 3 months after infection.¹⁶ Selective expression of the

Supported by the Ministry of Education, Culture, Sports, Science, and Technology; and the Ministry of Health, Labour, and Welfare, of Japan.

Accepted for publication March 21, 2006.

GenBank accession numbers: DQ399740, DQ399741, DQ399742.

Present address of H.I.: Hakodate Central General Hospital, Hakodate, Japan; present address of T.Y.: Genetic Lab Co. Ltd., Sapporo, Japan.

Address reprint requests to Akihiro Ishizu, Department of Pathology/Pathophysiology, Division of Pathophysiological Science, Hokkaido University Graduate School of Medicine, Kita-15, Nishi-7, Kita-ku, Sapporo 060-8638, Japan. E-mail: aishizu@med.hokudai.ac.jp.

HTLV-1 *pX* gene peaks 7 months after infection, accompanied by an increase in tumor necrosis factor- α levels in the spinal cord and down-regulation of the anti-apoptotic *bcl-2* gene in oligodendrocytes.^{17,18} Thus, we reasoned that the most crucial molecular events occurred ~7 months after HTLV-1 infection in our rat model.

The proinflammatory cytokine interferon (IFN)- γ , secreted from activated T and NK cells, increases MHC class I and II expression on a wide variety of cells and then induces a Th1-type immune response. Until recently, IFN- γ had been considered a deleterious factor for central nervous system (CNS) disorders such as multiple sclerosis and experimental autoimmune encephalomyelitis.^{19,20} However, several lines of evidence indicate that, in some instances, IFN- γ exerts protective effects against CNS disorders. First, inactivation of the *IFN- γ* gene by gene knockout converts an otherwise experimental autoimmune encephalomyelitis-resistant mouse strain to experimental autoimmune encephalomyelitis-susceptible.²¹ Second, a low level of IFN- γ expression in the CNS plays a protective role in cuprizone-induced demyelination.²² Third, BALB/c mice treated with an anti-IFN- γ antibody become susceptible to measles virus encephalitis, and viral clearance from the CNS is impaired.²³ Fourth, treatment with IFN- γ results in inhibition of viral replication in primary cultured nerve cells infected with measles virus.²⁴ Fifth, IFN- γ protects neurons from apoptosis during destructive encephalitis induced by herpes simplex virus type 1.²⁵ In these reports,²¹⁻²⁵ the authors assumed that IFN- γ was derived from mononuclear cells, including T and NK cells, infiltrating into the CNS.

We show here that IFN- γ levels in the spinal cord are significantly increased in HAM-resistant ACI and LEW rats 7 months after HTLV-1 infection, whereas no such increase occurs in HAM-susceptible WKAH rats. Infiltration of mononuclear cells was never seen in the CNS of HTLV-1-infected rats, indicating that IFN- γ was produced by resident cells of the CNS. By confocal laser-scanning microscopy, we identified IFN- γ -producing cells in the spinal cord of HAM-resistant rats as neurons. We suggest that IFN- γ produced by neurons in response to HTLV-1 infection has a protective role against the development of myelopathy.

Materials and Methods

Rats and HTLV-1 Infection

Inbred ACI, LEW, and WKAH rats were obtained from the Institute for Animal Experimentation, Hokkaido University Graduate School of Medicine. HTLV-1 infection was achieved as described.¹² Briefly, HTLV-1-immortalized MT-2²⁶ was injected into the peritoneal cavity of newborn rats (1×10^7 cells/rat). All HTLV-1-infected rats were maintained in the P3 room. At least three rats were used in each experiment. All rats used in this study were anesthetized with sodium pentobarbital and then intravascularly perfused with ice-cold saline. All animal experiments were done in accordance with the Guide for Care and

Use of Laboratory Animals in Hokkaido University Graduate School of Medicine.

Tissue Sampling for mRNA Extraction

After perfusion with ice-cold saline, the spinal cord, cerebrum, and spleen were harvested, flash-frozen in liquid nitrogen, and served as samples for mRNA extraction. Microglia- and neuron-rich populations were prepared from the spinal cord as follows: the harvested spinal cord was dissected and then incubated in RPMI 1640 medium (Sigma-Aldrich, St. Louis, MO) containing 0.25% collagenase (Worthington Biochemical Corp., Freehold, NJ) and 700 U DNase I (Takara, Otsu, Japan) for 30 minutes at 37°C. Microglia-rich populations were separated from the solution by Percoll-gradient centrifugation as described by Tomaru and colleagues¹⁷ and Jiang and colleagues.¹⁸ For separation of neuron-rich populations, myelin residues were removed from the solution by centrifugation at $6 \times g$ for 1 minute, and then neurons in the supernatant were collected by centrifugation at $36 \times g$ for 7 minutes. All samples were stored at -80°C until use.

Reverse Transcriptase-Polymerase Chain Reaction (RT-PCR) and Quantitative Real-Time RT-PCR

Total RNAs were extracted using Isogen (Nippon Gene, Tokyo, Japan) and purified using the RNeasy mini kit (Qiagen, Alameda, CA). The purified total RNAs were reverse-transcribed using the Super Script III first-strand synthesis system for RT-PCR (Invitrogen, Carlsbad, CA). Quantitative real-time RT-PCR was done with the cDNAs, SYBR Green I dye (SYBR Green PCR Master Mix; Qiagen), and the primer set for *IFN- γ* (sense: 5'-GATCCAGCACAAAGCTGTCA-3', anti-sense: 5'-GACTCCTTTCCGCTTCCTT-3'), *interferon regulatory factor 1 (IRF-1)* (sense: 5'-TGAAGCTGCAACAGATGAGG-3', anti-sense: 5'-AGCAAGTATCCCTTGCCATC-3'), *IL-12p40* (sense: 5'-AGGTGCGTTCCTCGTAGAGA-3', anti-sense: 5'-CCATTGCTGCATGATGAAT-3'), *IL-12 receptor $\beta 1$ (IL-12R $\beta 1$)* (sense: 5'-AGGTGCAGATTTCCCGTTTA-3', anti-sense: 5'-CAGCCCTGTTAAGCCAATG-3'), *IL-12 receptor $\beta 2$ (IL-12R $\beta 2$)* (sense: 5'-TGCCACCAATCCCAAACCTA-3', anti-sense: 5'-CCTGCTTCCTAGCACCTTGT-3'), *IL-23p19* (sense: 5'-CACCCTGGGAGACTCAACA-3', anti-sense: 5'-AGGATCTTGGAACGGAGAGA-3'), *IL-23 receptor (IL-23R)* (sense: 5'-TTGATGAATTGTGCCTCGTT-3', anti-sense: 5'-GTCTGCGCTGGATAGTTTC-3'), *IL-27* (sense: 5'-ACTCTGCTTCCTCGCTACCA-3', anti-sense: 5'-GGAGATCCAGCCTCATTGC-3'), *IL-27 receptor (IL-27R, WSX-1)* (sense: 5'-AGCCCAGGGATAAAGGTGAC-3', anti-sense: 5'-AGACGGGTCCAGTTGAGCTT-3'), or *GAPDH* (sense: 5'-ATGGGAGTTGCTGTTGAAGTCA-3', anti-sense: 5'-CCGAGGGCCCACTAAAGG-3'). PCR was performed in a two-step reaction (95°C for 30 seconds, 60°C for 30 seconds) for 45 cycles after initial denaturation (95°C, 15 minutes), using the ABI Prism 7000 sequence detector

system (Applied Biosystems, Foster City, CA). Relative expression of target genes was analyzed using the $\Delta\Delta$ CT-method.²⁷ The amount of specific mRNA was quantified at the point where the system detected uptake in the exponential phase of PCR accumulation and normalized to *GAPDH* mRNA levels.

Enzyme-Linked Immunosorbent Assay (ELISA)

ELISA for rat IFN- γ was performed using a kit (BioSource, Camarillo, CA). In brief, after perfusion with ice-cold saline, harvested spinal cords were homogenized with 1 ml of phosphate-buffered saline (PBS) containing 10 μ g/ml aprotinin, 1 μ g/ml leupeptin, and 1 μ g/ml phenylmethyl sulfonyl fluoride. Duplicate samples (100 μ l) of spinal cord homogenates were subjected to ELISA according to the manufacturer's instructions. The detection limit of the kit was 13 pg/ml.

Primary Culture of Rat Spinal Cord Cells

Saline-perfused spinal cords were obtained from rats 7 months after HTLV-1 infection and from age-matched control rats. Harvested spinal cords were dissected and digested as described above. Cell suspensions were centrifuged, and then the pellet was resuspended in 30% Percoll (Amersham Biosciences, Uppsala, Sweden) diluted with Hanks' balanced salt solution (Invitrogen, Carlsbad, CA). The cell suspension was laid gently on 80% Percoll solution. The gradient solution was centrifuged at 1800 $\times g$ for 40 minutes. Cells in the 30% Percoll layer were dissociated, washed, and then plated sparsely on poly-L-lysine-coated dishes in Dulbecco's modified Eagle's medium/Ham's F12 medium (Invitrogen) supplemented with 10% fetal calf serum and 50 ng/ml of nerve growth factor 2.5S (Invitrogen) at 37°C in an atmosphere of 5% CO₂.

Recombinant Cytokines

Recombinant rat IFN- γ was purchased from PeproTech EC (London, UK). Recombinant mouse interleukin (IL)-12, previously shown to function in rats,²⁸ was purchased from R&D Systems (Minneapolis, MN).

Immunofluorescent Staining

Cells cultured on poly-L-lysine/laminin-coated glasses for 5 days were fixed with 4% paraformaldehyde for 15 minutes. For intracellular staining, cells were treated with PBS containing 0.1% Triton-X and 0.05% bovine serum albumin for 4 minutes and then fixed with ice-cold 70% methanol for 4 minutes. Nonspecific binding was blocked with PBT (0.05% Tween-20/0.1% bovine serum albumin in PBS) containing 0.1% goat serum for 10 minutes. Primary antibodies used were mouse monoclonal anti-rat IFN- γ (DB1; PBL Biomedical Laboratories, Piscataway, NJ), mouse monoclonal anti-rat CD68 (ED-1; Serotec, Oxford, UK), rabbit polyclonal anti-neurofilament (NF)

150-kd molecule (AB1981; Chemicon International, Temecula, CA), and rabbit polyclonal anti-glial fibrillary acidic protein (GFAP) (Dakocytomation, Glostrup, Denmark). For double staining, cells were labeled with DB1 and AB1981, DB1 and anti-GFAP, or ED-1 and AB1981 followed by labeling with Alexa Fluor 488-conjugated goat polyclonal antibody to mouse IgG and Alexa Fluor 568-conjugated goat polyclonal antibody to rabbit IgG. Confocal images were acquired with a laser-scanning microscope (MRC-1024; Bio-Rad Laboratories, Hercules, CA).

Effects of IFN- γ on HTLV-1 Gene Expression

LEW-S1,¹² an HTLV-1-immortalized rat T-cell line, was incubated with 100 or 1000 U/ml recombinant rat IFN- γ for 3 hours, and the relative expression of the HTLV-1 *pX* gene to the structural *gag* gene was calculated using the quantitative real-time RT-PCR method. Primer sets used were 5'-ATCCCGTGGAGACTCCTCAA-3' (sense) and 5'-CCAAACACGTAGACTGGGTATCC-3' (anti-sense) for *pX* and 5'-CCAATGCAAACAAAGAATGC-3' (sense) and 5'-AGCCCGCAACATATCTCCTA-3' (anti-sense) for *gag*.

Sequencing of the 5'-Flanking Region of the Rat IL-12R β 2 Gene

Genomic DNA was extracted from the tails of ACI, LEW, and WKAH rats using the DNeasy tissue kit (Qiagen). The 5'-flanking region of the *IL-12R β 2* gene (1.8 kb) was amplified by nested PCR (outer primers, 5'-ACCACACCTCTTGCCATTTT-3' and 5'-CGAATCGGAGTACACTGCTG-3'; inner primers, 5'-CCCAGAGGCACTTTAAGCA-3' and 5'-ACCGATGGACAATGGGTATC-3'). After gel electrophoresis, the PCR products were purified with Freeze 'N Squeeze DNA gel extraction spin columns (Bio-Rad Laboratories) and subjected to direct sequencing with the CEQ 2000XL DNA analysis system (Beckman-Coulter, Fullerton, CA). Sequences were aligned using the online ClustalW service (<http://www.ddbj.nig.ac.jp/search/clustalw-j.html>) and potential binding sites of transcription factors were identified using the Transfac database (<http://motif.genome.jp/>).

Statistical Analysis

Data were analyzed with either Student's *t*-test or repeated measures analysis of variance, appropriately. *P* values less than 0.05 were considered to be significant.

Results

HTLV-1 Infection Induces IFN- γ Production in the Spinal Cord of HAM-Resistant but Not HAM-Susceptible Rats

In view of the fact that IFN- γ exerts protective effects against CNS disease,²¹⁻²⁵ we compared the expres-

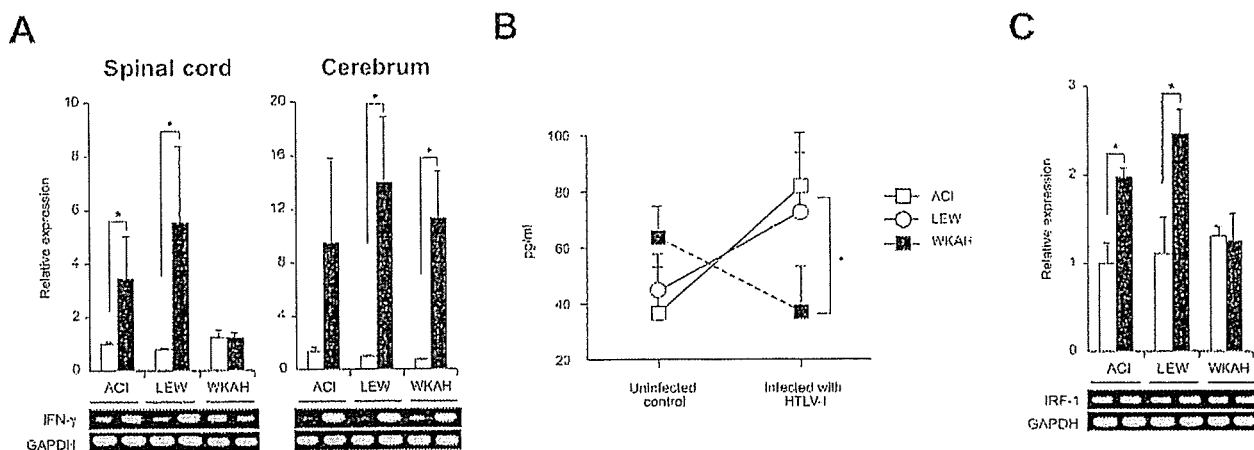


Figure 1. A: The amount of *IFN-γ* mRNA in the spinal cord and cerebrum was quantified by real-time RT-PCR. Samples were obtained from rats 7 months after HTLV-1 infection (black columns) and from age-matched uninfected controls (white columns). Results of experiments done in triplicate were evaluated as relative expression levels to the *GAPDH* gene. Data are represented as mean \pm SD values of experiments done independently three times. Representative photos of gel electrophoresis of RT-PCR products are shown beneath the graph. B: The amount of *IFN-γ* protein in the spinal cord was quantified using the ELISA kit. Samples were obtained from rats 7 months after HTLV-1 infection and from age-matched uninfected controls. Data are represented as mean \pm SD values of experiments done independently three times. C: The amount of *IRF-1* mRNA in the spinal cord was quantified by real-time RT-PCR. Samples were obtained from rats 7 months after HTLV-1 infection (black columns) and from age-matched uninfected controls (white columns). Results of experiments done in triplicate were evaluated as relative expression levels to the *GAPDH* gene. Data are represented as mean \pm SD values of experiments done independently three times. Representative photos of gel electrophoresis of RT-PCR products are shown beneath the graph. In each group of all experiments, at least three rats were used. * $P < 0.05$.

sion levels of *IFN-γ* mRNA between HAM-susceptible and -resistant rats 7 months after inoculation with HTLV-1 (Figure 1). Expression of *IFN-γ* was quantified by real-time RT-PCR in the spinal cord, cerebrum, and spleen. We used tissue samples obtained 7 months after infection because our previous work indicated that critical molecular events leading to the development of HAM rat disease occurred at this time period.^{17,18,29}

The expression of *IFN-γ* in the spinal cord, an organ affected in HAM rat disease, was significantly elevated in HAM-resistant ACI and LEW rats compared with age-matched, uninfected controls, whereas the expression levels of *IFN-γ* in the spinal cord of HAM-susceptible WKAH rats were almost the same as those in uninfected controls (Figure 1A, left). The expression of *IFN-γ* in the cerebrum, an organ never affected in HAM rat disease, was remarkably increased in infected rats regardless of whether they were HAM-resistant or -susceptible (Figure 1A, right). In spleen cells, the mRNA level of *IFN-γ* did not change by infection; however, even in the absence of infection, *IFN-γ* was expressed more abundantly than in the cerebrum of infected rats (data not shown). Increased expression of *IFN-γ* mRNA was not evident in the spinal cord of HAM-resistant rats 3 months after infection, when the provirus was barely detected (data not shown).

To evaluate expression of *IFN-γ* at the protein level, spinal cords were harvested from infected and age-matched uninfected rats and the tissue extracts subjected to assay using an ELISA kit. Consistent with the results obtained at the mRNA level, the amount of *IFN-γ* proteins in the spinal cord was increased in HAM-resistant ACI and LEW rats but not in HAM-susceptible WKAH rats when measured 7 months after HTLV-1 infection (Figure 1B).

We next examined expression of the *IRF-1* gene. *IRF-1* is known as a downstream molecule induced by *IFN-γ*.³⁰ Like *IFN-γ*, expression of *IRF-1* was significantly increased in the spinal cord of ACI and LEW rats 7 months after infection, whereas no such increase was seen in the spinal cord of WKAH rats (Figure 1C). Thus, collective evidence clearly indicated that *IFN-γ* was induced by HTLV-1 infection only in the spinal cords of HAM-resistant strains.

IFN-γ Suppresses *pX* Gene Expression in Cultured HTLV-1-Immortalized Rat Cells

IFN-γ was recently shown to have a negative regulatory role against HTLV-1 gene expression.³¹ To examine whether *IFN-γ* can suppress expression of the *pX* gene, previously shown to play a critical role in the

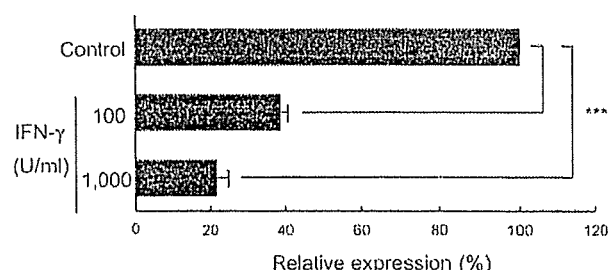


Figure 2. The HTLV-1-immortalized rat T-cell line, LEW-S1, was incubated with 100 or 1000 U/ml of recombinant rat *IFN-γ* for 3 hours, and then expression of the *pX* gene was quantified using the real-time RT-PCR method. Results of experiments done in triplicate were evaluated as relative expression levels to the structural *gag* gene. Data are represented as mean \pm SD values of experiments done independently three times. *** $P < 0.0001$.

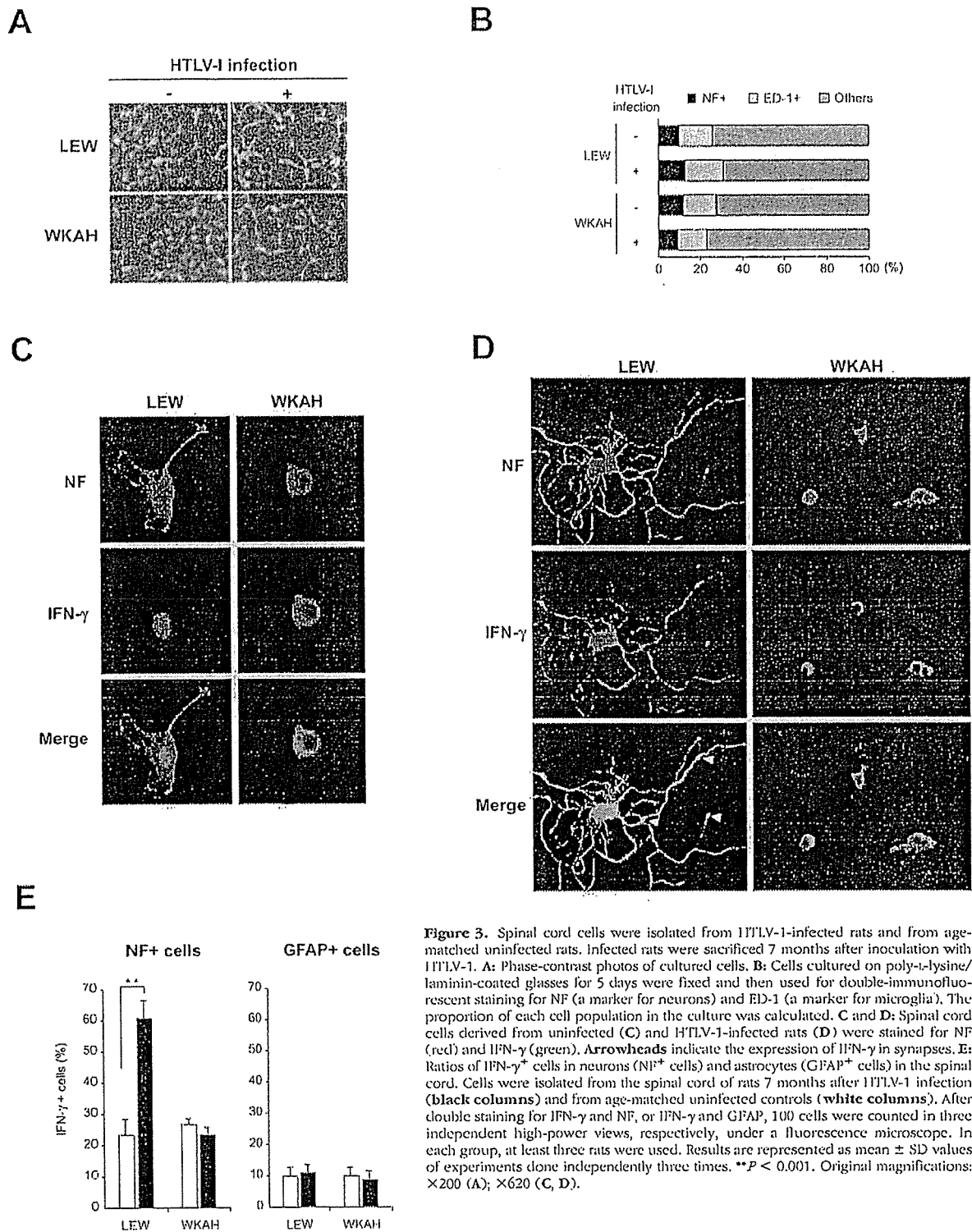


Figure 3. Spinal cord cells were isolated from HTLV-1-infected rats and from age-matched uninfected rats. Infected rats were sacrificed 7 months after inoculation with HTLV-1. **A:** Phase-contrast photos of cultured cells. **B:** Cells cultured on poly-L-lysine/laminin-coated glasses for 5 days were fixed and then used for double-immunofluorescent staining for NF (a marker for neurons) and ED-1 (a marker for microglia). The proportion of each cell population in the culture was calculated. **C and D:** Spinal cord cells derived from uninfected (**C**) and HTLV-1-infected rats (**D**) were stained for NF (red) and IFN- γ (green). **Arrowheads** indicate the expression of IFN- γ in synapses. **E:** Ratios of IFN- γ + cells in neurons (NF+ cells) and astrocytes (GFAP+ cells) in the spinal cord. Cells were isolated from the spinal cord of rats 7 months after HTLV-1 infection (black columns) and from age-matched uninfected controls (white columns). After double staining for IFN- γ and NF, or IFN- γ and GFAP, 100 cells were counted in three independent high-power views, respectively, under a fluorescence microscope. In each group, at least three rats were used. Results are represented as mean \pm SD values of experiments done independently three times. ** $P < 0.001$. Original magnifications: $\times 200$ (**A**); $\times 620$ (**C, D**).

onset of HAM rat disease,^{17,18} we treated the HTLV-1-immortalized rat T-cell line LEW-S1¹² with IFN- γ for 3 hours *in vitro* and then monitored expression of the *pX* gene by real-time RT-PCR (Figure 2). Expression of the *pX* gene relative to that of the structural *gag* gene was decreased in response to IFN- γ in a dose-dependent

manner. These results suggest that IFN- γ is likely to protect against the development of HAM rat disease by down-regulating *pX* gene expression. Thus, WKAH rats presumably develop HAM rat disease because their spinal cord cells cannot produce IFN- γ in response to HTLV-1 infection.

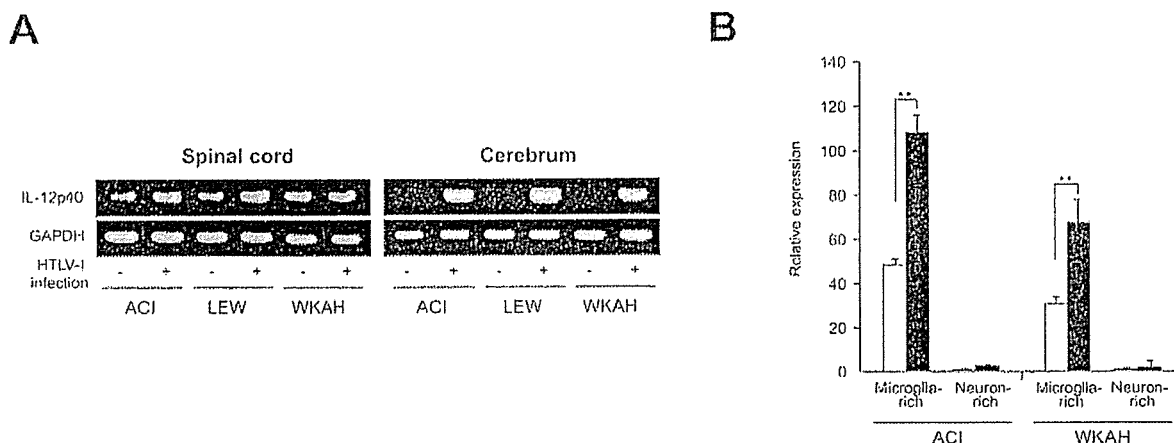


Figure 4. **A:** Expression of the *IL-12p40* gene in the spinal cord and cerebrum. Samples were obtained from rats 7 months after HTLV-1 infection and from age-matched uninfected controls. Experiments were repeated independently at least three times. Representative photos of gel electrophoresis of RT-PCR products are shown. **B:** The amount of *IL-12p40* mRNA in microglia- or neuron-rich populations prepared from the spinal cord was quantified by real-time RT-PCR. Samples were obtained from rats 7 months after HTLV-1 infection (black columns) and from age-matched uninfected controls (white columns). Data (relative expression levels to the *GAPDH* gene) are represented as mean \pm SE values obtained from experiments performed in triplicate and repeated three times. In each group, at least three rats were used. ** $P < 0.001$.

Cells that Produce IFN- γ in the Spinal Cord of HTLV-1-Infected HAM-Resistant Rats Are Neurons

To identify IFN- γ -producing cells, we established primary cultures of rat spinal cord cells from both LEW and WKAH strains (Figure 3A). These cells were observed under a confocal laser-scanning microscope after immunofluorescent double staining for NF and ED-1. The cultured cells prepared from both strains, infected and uninfected, contained a nearly equivalent proportion of NF⁺ neurons, ED-1⁺ microglia, and other glial cells (Figure 3B), thus ensuring that the samples subjected to comparison were not substantially different in terms of cell populations.

We stained the cells with antibodies for NF and IFN- γ , or for GFAP and IFN- γ , and focused our analysis on neurons and astrocytes because they are known to express IFN- γ in the CNS.³²⁻³⁴ Weak expression of IFN- γ was seen in the perinuclear cytoplasm of NF⁺ neurons derived from uninfected LEW and WKAH rats (Figure 3C). The neurons obtained from LEW rats infected with HTLV-1 showed intense immunoreactivity to IFN- γ not only in the perinuclear cytoplasm but also in the dendrites, whereas HTLV-1 infection did not cause any significant alteration in the staining pattern or morphology in the neurons of WKAH rats as compared with those of uninfected control rats (Figure 3D). Neurite outgrowth was markedly induced by HTLV-1 infection in LEW but not WKAH rats. IFN- γ treatment is known to induce differentiation of neurons and an outgrowth of dendrites.³⁵ Thus, the morphological alterations seen in Figure 3, C and D, are consistent with the observation that HTLV-1 infection induced IFN- γ expression in the spinal cord of HAM-resistant but not HAM-susceptible rats (Figure 1). We presume that IFN- γ produced by neurons of LEW rats acts in an autocrine and/or paracrine manner and promotes their differentiation and neurite outgrowth. Interestingly,

IFN- γ induced in the neurons of HTLV-1-infected LEW rats appeared to accumulate in synaptic junctions (Figure 3D, arrowheads). This is in line with the observation that the receptors for IFN- γ are expressed at synapses in the superficial dorsal horn and lateral spinal nucleus³⁶ and suggests that IFN- γ produced in neurons might function as a neurotransmitter in the CNS. On the other hand, the expression of IFN- γ in GFAP⁺ astrocytes was weak regardless of whether they originated from infected or uninfected animals or from HAM-susceptible or -resistant strains (data not shown). Quantitative analysis based on cell counting confirmed that neurons rather than astrocytes were the major IFN- γ -producing cells in the spinal cord of infected rats (Figure 3E).

Spinal Cord Cells of HAM-Susceptible Rats Do Not Produce IFN- γ in Response to IL-12

Certain infections induce production of IL-12, which in turn promotes production of IFN- γ .³⁷ Our RT-PCR experiments showed that HTLV-1 infection induced expression of *IL-12p40* mRNA in the cerebrum of both HAM-resistant and -susceptible strains (Figure 4A, right). Induction of *IL-12p40* was not obvious when the whole spinal cord samples were subjected to analysis (Figure 4A, left); however, when they were fractionated into microglia- and neuron-rich populations, we could clearly see elevated expression of *IL-12p40* in the former, but not in the latter, populations (Figure 4B). These findings are consistent with our previous observation that the HTLV-1 provirus was localized to microglia and macrophages.¹⁶ Basal *IL-12p40* mRNA levels in the microglia-rich population were lower in WKAH than in ACI rats. However, in both strains, HTLV-1 infection almost doubled the expression levels of *IL-12p40* in microglia-rich populations (Figure 4B). We thus reasoned that the failure of WKAH spinal cord cells to produce IFN- γ is unlikely to be caused by defective induction of IL-12.

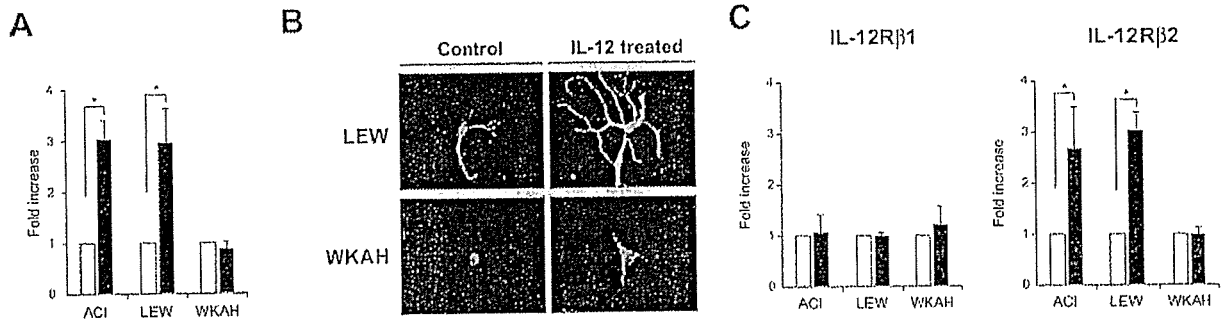


Figure 5. **A:** The amount of *IFN- γ* mRNA in the cells isolated from the spinal cord of uninfected rats was quantified by real-time RT-PCR. Samples were obtained from the cells after treatment with recombinant IL-12 (100 ng/ml) for 18 hours (black columns). Results of experiments done in triplicate and repeated three times were evaluated as mean \pm SE values of the fold increase to the data without IL-12 treatment (white columns). * $P < 0.05$. **B:** Cells isolated from the spinal cord of uninfected rats were cultured on poly-L-lysine/laminin-coated glasses. After incubation with recombinant IL-12 (100 ng/ml) for 5 days, immunofluorescent double staining was performed using anti-IFN- γ (green) and anti-NF (red) antibodies. Representative merged images are shown. Experiments were performed independently three times. **C:** The amount of *IL-12R β 1* and *IL-12R β 2* mRNAs in the cells isolated from the spinal cord of uninfected rats was quantified by real-time RT-PCR. Samples were obtained from the cells after treatment with recombinant IL-12 (100 ng/ml) for 18 hours (black columns). Results of experiments done in triplicate and repeated three times were evaluated as mean \pm SE values of the fold increase to the data without IL-12 treatment (white columns). * $P < 0.05$. For all experiments, at least three rats were used in each group. Original magnifications, $\times 620$ (B).

We then tested the possibility that the inability of WKAH rats to produce IFN- γ in their spinal cords is caused by defective response to IL-12. To this end, primary culture cells from the spinal cord of uninfected rats were treated with IL-12 *in vitro*, and then expression of *IFN- γ* was examined. By exposure to IL-12 for 18 hours, expression levels of *IFN- γ* were markedly increased in tissue-cultured spinal cord cells from HAM-resistant ACI and LEW rats, whereas no alteration was seen in the cells from HAM-susceptible WKAH rats (Figure 5A).

We confirmed by immunofluorescent staining that treatment with IL-12 induced IFN- γ only in the neurons of HAM-resistant rats (Figure 5B). IL-12 also induced neurite outgrowth in neurons prepared from LEW rats, presumably through the actions of IFN- γ . By contrast, similar treatment did not induce neurite outgrowth in WKAH rats. Thus, the unresponsiveness of WKAH-derived neurons to IL-12 *in vitro* closely mirrored the inability of WKAH-derived neurons to produce IFN- γ and undergo neurite outgrowth in response to HTLV-1 infection (Figures 1 and 3).

Spinal Cord Cells from HAM-Susceptible Rats Do Not Show Elevated *IL-12R β 2* Expression in Response to IL-12

To understand why WKAH neurons do not respond to IL-12, we examined expression of IL-12 receptors in tissue-cultured spinal cord cells obtained from HAM-resistant and -susceptible strains. IL-12 receptors are composed of $\beta 1$ and $\beta 2$ subunits.³⁸ Although *IL-12R β 1* is expressed constitutively, expression of *IL-12R β 2* is up-regulated by IL-12. Expression levels of *IL-12R β 1* mRNA were not altered by IL-12 treatment in HAM-resistant or -susceptible strains (Figure 5C, left). By contrast, treatment with IL-12 markedly increased *IL-12R β 2* mRNA in spinal cord cells from ACI and LEW but not from WKAH rats (Figure 5C, right). These results indicate that the absence of IFN- γ pro-

duction in the spinal cord of WKAH rats results from inability of the *IL-12R β 2* gene to respond to IL-12 signals.

WKAH ACI LEW	-1679 -1679 -1679	CTCTACTTAA CTCTACTTAA CTCTACTTAA	ACAAGCAGCC ACAAGCAGCC ACAAGCAGCC	ACCTTCAGAG ACCTTCAGAG ACCTTCAGAG	GCGAGGAGTA GCGAGGAGTA GCGAGGAGTA	GGAAGAGTAA GGAAGAGTAA GGAAGAGTAA	GCGATYACCA GCGATYACCA GCGATYACCA
WKAH ACI LEW	-1613 -1613 -1613	TAGAGTTCCT TAGAGTTCCT TAGAGTTCCT	CAGTCGPDAA CAGTCGPDAA CAGTCGPDAA	AAACAGCTCAG AAACAGCTCAG AAACAGCTCAG	ACTTCGCTAG ACTTCGCTAG ACTTCGCTAG	AAAGAGCTCA AAAGAGCTCA AAAGAGCTCA	TTCATYAAA TTCATYAAA TTCATYAAA
WKAH ACI LEW	-1654 -1654 -1654	ACTTCTTAAG ACTTCTTAAG ACTTCTTAAG	TCTGGGAAA TCTGGGAAA TCTGGGAAA	GTTCGAGAA GTTCGAGAA GTTCGAGAA	TTCGAGAGC TTCGAGAGC TTCGAGAGC	TGAAAGATTC TGAAGATTC TGAAGATTC	TTCATYAAA TTCATYAAA TTCATYAAA
WKAH ACI LEW	-1693 -1693 -1693	AAGAGATAG AAGAGATAG AAGAGATAG	GCCTCTTTC GCCTCTTTC GCCTCTTTC	AAAGAGCTCA AAAGAGCTCA AAAGAGCTCA	ATTGAGCTC ATTGAGCTC ATTGAGCTC	ATGAAATCTT ATGAAATCTT ATGAAATCTT	ATGAGCTTT ATGAGCTTT ATGAGCTTT
WKAH ACI LEW	-1633 -1633 -1633	CAAGCTTGG CAAGCTTGG CAAGCTTGG	CCCCATTTT CCCCATTTT CCCCATTTT	GGAGTTCCT GGAGTTCCT GGAGTTCCT	AAAGAGCTCA AAAGAGCTCA AAAGAGCTCA	GAGCAGGCA GAGCAGGCA GAGCAGGCA	AGCCATGAG AGCCATGAG AGCCATGAG
WKAH ACI LEW	-1713 -1713 -1713	AGCCCTTTC AGCCCTTTC AGCCCTTTC	TCTTGGAGC TCTTGGAGC TCTTGGAGC	TAAAGCTCAG TAAAGCTCAG TAAAGCTCAG	GAAGAGCTCA GAAGAGCTCA GAAGAGCTCA	GATGAGAGCA GATGAGAGCA GATGAGAGCA	ATGATYAT ATGATYAT ATGATYAT
WKAH ACI LEW	-1719 -1719 -1719	GGATAGCTAT GGATAGCTAT GGATAGCTAT	TAGAGAGAT TAGAGAGAT TAGAGAGAT	GGTTCAGTCA GGTTCAGTCA GGTTCAGTCA	CTCTGATTC CTCTGATTC CTCTGATTC	AAAGATTCG AAAGATTCG AAAGATTCG	ATGAGCTTT ATGAGCTTT ATGAGCTTT
WKAH ACI LEW	-1659 -1659 -1659	ACTTGAACA ACTTGAACA ACTTGAACA	TGATTTACT TGATTTACT TGATTTACT	TGATTTGGA TGATTTGGA TGATTTGGA	GAATTCAGC GAATTCAGC GAATTCAGC	AACTTGTCTA AACTTGTCTA AACTTGTCTA	TAGCAGGAT TAGCAGGAT TAGCAGGAT
WKAH ACI LEW	-1699 -1699 -1699	GTCCAGGCT GTCCAGGCT GTCCAGGCT	CTGAGCAGC CTGAGCAGC CTGAGCAGC	TGTTTAAAG TGTTTAAAG TGTTTAAAG	GAGCTTCAG GAGCTTCAG GAGCTTCAG	ATGAAATTTA ATGAAATTTA ATGAAATTTA	AGGCTATCT AGGCTATCT AGGCTATCT
WKAH ACI LEW	-1539 -1539 -1539	TGATATCTC TGATATCTC TGATATCTC	TGCAATAGA TGCAATAGA TGCAATAGA	CTTACTAGAG CTTACTAGAG CTTACTAGAG	AAATTAAGT AAATTAAGT AAATTAAGT	AGCAATCTTA AGCAATCTTA AGCAATCTTA	AGGCTATCT AGGCTATCT AGGCTATCT
WKAH ACI LEW	-1619 -1619 -1619	GGAGATTCG GGAGATTCG GGAGATTCG	TATTCATAT TATTCATAT TATTCATAT	GGTTCAGTCT GGTTCAGTCT GGTTCAGTCT	TCCAGTTCG TCCAGTTCG TCCAGTTCG	AGCCATAGCA AGCCATAGCA AGCCATAGCA	AACTTGTCT AACTTGTCT AACTTGTCT
WKAH ACI LEW	-1419 -1419 -1419	GAAGAGCTC GAAGAGCTC GAAGAGCTC	GGGCTTCAG GGGCTTCAG GGGCTTCAG	TTCGCTTCG TTCGCTTCG TTCGCTTCG	GAGATTCAG GAGATTCAG GAGATTCAG	CTGAGCAGC CTGAGCAGC CTGAGCAGC	CTTATGAA CTTATGAA CTTATGAA
WKAH ACI LEW	-1514 -1514 -1514	TGTTTATG TGTTTATG TGTTTATG	TCCGAGGAG TCCGAGGAG TCCGAGGAG	TGAGAGGAA TGAGAGGAA TGAGAGGAA	GAAGAGCTC GAAGAGCTC GAAGAGCTC	AACTTGTCTA AACTTGTCTA AACTTGTCTA	TAGCAGGAT TAGCAGGAT TAGCAGGAT
WKAH ACI LEW	-1699 -1699 -1699	CAAGCTTAA CAAGCTTAA CAAGCTTAA	ATAGAAATC ATAGAAATC ATAGAAATC	TAGCAGCTT TAGCAGCTT TAGCAGCTT	ATTTCATTA ATTTCATTA ATTTCATTA	AACTTGTCTA AACTTGTCTA AACTTGTCTA	TTCATYAT TTCATYAT TTCATYAT
WKAH ACI LEW	-1614 -1614 -1614	AGGCTCTCA AGGCTCTCA AGGCTCTCA	AGGAGCTTT AGGAGCTTT AGGAGCTTT	AAAGAGCTC AAAGAGCTC AAAGAGCTC	AAAGAGCTC AAAGAGCTC AAAGAGCTC	AACTTGTCTA AACTTGTCTA AACTTGTCTA	TAGCAGGAT TAGCAGGAT TAGCAGGAT
WKAH ACI LEW	-1113 -1113 -1113	CAAGAGCTC CAAGAGCTC CAAGAGCTC	CTAGAGCAG CTAGAGCAG CTAGAGCAG	TAGTTCAGG TAGTTCAGG TAGTTCAGG	TGCTTCAGG TGCTTCAGG TGCTTCAGG	CAAGAGCTC CAAGAGCTC CAAGAGCTC	GGTTCATCT GGTTCATCT GGTTCATCT
WKAH ACI LEW	-1113 -1113 -1113	TGATTTATG TGATTTATG TGATTTATG	TAGGAGGAG TAGGAGGAG TAGGAGGAG	TGCTTCAGG TGCTTCAGG TGCTTCAGG	TGCTTCAGG TGCTTCAGG TGCTTCAGG	CAAGAGCTC CAAGAGCTC CAAGAGCTC	GGTTCATCT GGTTCATCT GGTTCATCT
WKAH ACI LEW	-1113 -1113 -1113	TGATTTATG TGATTTATG TGATTTATG	TAGGAGGAG TAGGAGGAG TAGGAGGAG	TGCTTCAGG TGCTTCAGG TGCTTCAGG	TGCTTCAGG TGCTTCAGG TGCTTCAGG	CAAGAGCTC CAAGAGCTC CAAGAGCTC	GGTTCATCT GGTTCATCT GGTTCATCT
WKAH ACI LEW	-1113 -1113 -1113	TGATTTATG TGATTTATG TGATTTATG	TAGGAGGAG TAGGAGGAG TAGGAGGAG	TGCTTCAGG TGCTTCAGG TGCTTCAGG	TGCTTCAGG TGCTTCAGG TGCTTCAGG	CAAGAGCTC CAAGAGCTC CAAGAGCTC	GGTTCATCT GGTTCATCT GGTTCATCT
WKAH ACI LEW	-1113 -1113 -1113	TGATTTATG TGATTTATG TGATTTATG	TAGGAGGAG TAGGAGGAG TAGGAGGAG	TGCTTCAGG TGCTTCAGG TGCTTCAGG	TGCTTCAGG TGCTTCAGG TGCTTCAGG	CAAGAGCTC CAAGAGCTC CAAGAGCTC	GGTTCATCT GGTTCATCT GGTTCATCT

Figure 6. The 5'-flanking region of the rat *IL-12R β 2* gene. The genomic DNA was extracted from the tail of HAM-susceptible (WKAH) and HAM-resistant (ACI, LEW) rats, and then the 5'-flanking region of the *IL-12R β 2* gene was amplified by nested PCR. The PCR products were purified and subjected to direct sequencing. Shaded sequences represent potential SP-1 or GATA-3 binding sites. +1 represents a tentatively assigned transcription start site deduced from the data available for the mouse *IL-12R β 2* gene.

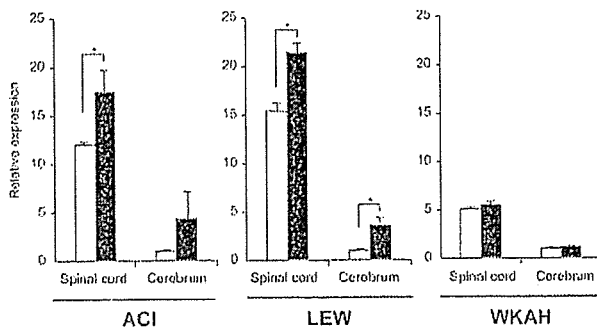


Figure 7. The amount of *IL-12Rβ2* mRNA in the spinal cord and cerebrum was quantified by real-time RT-PCR. Samples were obtained from rats 7 months after HTLV-1 infection (black columns) and from age-matched uninfected controls (white columns). Results of experiments performed in triplicate were evaluated as relative expression levels to the *GAPDH* gene. For each strain, the expression level of *IL-12Rβ2* mRNA in the cerebrum of uninfected control rats was set as 1. Relative expression levels (mean ± SD values) were determined from the experiments done independently three times. In each group, at least three rats were used. **P* < 0.05.

The 5'-Flanking Region of the Rat *IL-12Rβ2* Gene Is Polymorphic

To examine whether the defect is in the *IL-12Rβ2* gene itself, we compared its 5'-flanking sequence between HAM-resistant and -susceptible strains. Although HAM-resistant ACI and LEW rats had an identical sequence, the sequence of HAM-susceptible WKAH rats differed from that of ACI and LEW rats by 5 bp in the region spanning -1079 to -1 (Figure 6). We focused our analysis on SP-1 and GATA-3 binding sites because expression of the *IL-12Rβ2* gene has been shown to be regulated positively and negatively by SP-1 and GATA-3 transcription factors, respectively.^{39,40} None of the 5-bp substitutions affects potential SP-1 binding sites; however, the substitution from A to C at nucleotide position -239 generates an additional potential GATA-3 binding site in the WKAH sequence. As a result, there are three potential GATA-3 binding sites in WKAH, whereas ACI and LEW have only two such sites. Because GATA-3 is known to repress *IL-12Rβ2* gene expression strongly,⁴⁰ the single nucleotide polymorphism at nucleotide position -239 may be related to the defective induction of *IL-12Rβ2* transcription in WKAH rats.

In HAM-Susceptible Rats, HTLV-1 Infection Elevates mRNA Expression of *IL-23*, *IL-27*, and Their Receptors in the Cerebrum but Not in the Spinal Cord

In line with the *in vitro* studies, HTLV-1 infection did not induce *IL-12Rβ2* mRNA in the spinal cord or the cerebrum in WKAH rats (Figure 7). By contrast, HTLV-1 infection elevated *IL-12Rβ2* mRNA in both the spinal cord and cerebrum in HAM-resistant ACI and LEW rats. In WKAH rats, defective induction of *IL-12Rβ2* mRNA was observed not only in the spinal cord, but also in the cerebrum (Figure 7). This raised the question of why IFN-γ was induced in the cerebrum of WKAH rats 7 months after HTLV-1 infection (Figure 1A). To answer this question, we focused our analysis on *IL-23* and *IL-27* because these cytokines are known to induce IFN-γ.⁴¹ *IL-23* is composed of p19 and p40 subunits,⁴² and the p40 subunit is shared by *IL-12*. *IL-23* receptors are made up of *IL-12Rβ1* and the specific subunit, *IL-23R*. Expression levels of *IL-23p19*, *IL-12Rβ1*, *IL-23R*, *IL-27*, and *IL-27R* (*WSX-1*) genes were significantly increased in the cerebrum but not in the spinal cord of WKAH rats 7 months after HTLV-1 infection (Figure 8). These observations indicate that IFN-γ was induced in the cerebrum of WKAH rats through the *IL-23* and/or *IL-27* pathways.

Discussion

In the present study, we have demonstrated that expression of the proinflammatory cytokine IFN-γ is significantly elevated in the spinal cord of HAM-resistant rats 7 months after HTLV-1 infection (Figure 1). The increased expression of IFN-γ in the spinal cord was seen only in HAM-resistant strains. Importantly, we found that IFN-γ could suppress expression of the *pX* gene *in vitro* (Figure 2), the gene previously shown to be critically involved in the development of myelopathy in WKAH rats.^{17,18} Thus, combined evidence argues strongly that IFN-γ prevents the development of myelopathy by down-regulating *pX* gene expression in the spinal cord. However, there may be other mechanisms through which IFN-γ exerts protective effects against HAM rat disease. For example, IFN-γ is known to protect cord blood mononuclear cells from HTLV-1 infection when they are co-cultured with an

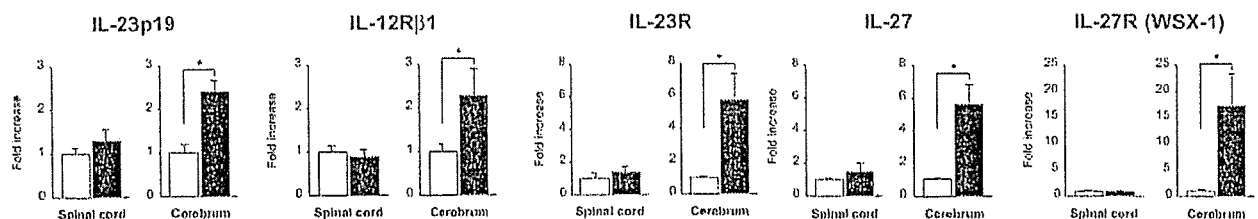


Figure 8. The amounts of *IL-23p19*, *IL-12Rβ1*, *IL-23R*, *IL-27*, and *IL-27R* (*WSX-1*) mRNAs in the spinal cord and cerebrum were quantified by real-time RT-PCR. Samples were obtained from WKAH rats 7 months after HTLV-1 infection (black columns) and from age-matched uninfected controls (white columns). In each group, at least three rats were used. Results of experiments done in triplicate were evaluated as relative expression levels to the *GAPDH* gene. Data from experiments done independently three times are represented as the fold increase (mean ± SD values) to the data without infection (white columns). **P* < 0.05.

HTLV-1-immortalized T-cell line MT-2, without altering the provirus load in the culture.³¹ Thus, IFN- γ may protect against the development of myelopathy through multiple mechanisms.

The CNS including the spinal cord has been considered as an absolute immunologically privileged site because of multiple anatomical and biochemical barriers known as blood-brain barriers. However, throughout the past decade, this view has been challenged by a number of observations showing that resident cells of the CNS produce cytokines and that such cytokines affect both proliferation and differentiation of cells in the CNS even under physiological conditions.⁴³ In the 1990s, it was suggested that endogenous IFN- γ exists in the CNS.⁴⁴ Endogenous IFN- γ was detected in the CNS of mice infected with Theiler's virus,⁴⁵ and Kiefer and colleagues⁴⁶ showed that IFN- γ was produced by rat neurons. Because there was no inflammatory cell infiltration in the CNS of HTLV-1-infected rats, our present study makes a strong case for the production of cytokines by CNS-resident cells. Neurons are not the sole source of IFN- γ in the CNS. Astrocytes in primary culture are known to produce and release IFN- γ after the mechanical and ischemic injuries.⁴⁷ It is also known that cultured rat astrocytes secrete IFN- γ in response to tumor necrosis factor- α in a dose-dependent manner.⁴⁸ We therefore asked which population of cells produced IFN- γ in the CNS of HTLV-1-infected, HAM-resistant rats. The observation made under a confocal microscope provided convincing evidence that neurons were the major cells that produced IFN- γ in our rat model of myelopathy (Figure 3). This is the first report demonstrating that HTLV-1 infection induces production of IFN- γ by neurons.

To understand why HTLV-1 infection failed to induce production of neuronal IFN- γ in the spinal cord of WKAH rats (Figures 1 and 3), we initially turned our attention to IL-12, an innate cytokine induced early during certain viral infections and a potent stimulator of IFN- γ .³⁷ This cytokine is secreted mainly from microglia in the CNS,⁴⁹ and in HTLV-1-infected rats, the provirus is predominantly localized in microglia and macrophages.¹⁶ We therefore assumed that infected microglia and/or macrophages in the CNS were the most likely source of IL-12. Consistent with this assumption, we detected *IL-12p40* mRNA in microglia-rich populations (Figure 4B). To examine whether poor induction of IL-12 after infection is responsible for the failure of WKAH rats to produce IFN- γ in their spinal cord neurons, we compared induction kinetics of *IL-12p40* mRNA between HAM-resistant and -susceptible strains (Figure 4B). In both ACI and WKAH strains, HTLV-1 infection elevated the amount of *IL-12p40* mRNA almost twofold in the microglia-rich population. Thus, the ability to produce IL-12 in response to infection is apparently not impaired in WKAH rats.

We then examined the possibility that WKAH rats might have a defect in its ability to respond to IL-12. To this end, cultured spinal cord cells from uninfected rats were treated with IL-12 *in vitro*, and then expression of IFN- γ was evaluated by real-time RT-PCR and by immunofluorescent staining (Figure 5). These experiments showed that IFN- γ induction by IL-12 occurs only in neurons

obtained from the spinal cords of HAM-resistant strains (Figure 5), indicating that signaling through the IL-12 receptor is defective in WKAH.

To examine whether the defect lies in the *IL-12R β 2* gene itself, we compared its 5'-flanking sequence between HAM-resistant and -susceptible strains. The two HAM-resistant strains, ACI and LEW, had an identical sequence; however, the sequence of WKAH rats differed from that of ACI and LEW by 5 bp (Figure 6). Interestingly, the A to C substitution at nucleotide position -239 generates an additional potential GATA-3 binding site in WKAH rats. Although the mechanism regulating the expression of the *IL-12R β 2* gene is only poorly understood, GATA-3 is known to repress its expression strongly.⁴⁰ Thus, the single nucleotide polymorphism at nucleotide position -239 may be involved in the defective induction of the *IL-12R β 2* gene in WKAH rats. However, functional studies are required to understand whether this polymorphism is biologically significant.

In WKAH rats, HTLV-1 infection did not up-regulate *IL-12R β 2* gene expression in the cerebrum (Figure 7). This observation was initially puzzling because the cerebrum of WKAH rats was able to produce IFN- γ in response to HTLV-1 infection (Figure 1A). A solution to this apparent paradox came from the fact that production of IFN- γ is regulated not only by IL-12 but also by IL-23 and IL-27.⁴¹ We observed that HTLV-1 infection increased the amount of mRNA for IL-23, IL-27, and their receptors in the cerebrum but not in the spinal cord of WKAH rats (Figure 8). Thus, alternative pathways of IFN- γ induction are active in the cerebrum of WKAH rats. We suggest that induction of IFN- γ via IL-12-independent pathways explains at least in part why the cerebrum is never affected in HAM rat disease.

In conclusion, this study is the first to indicate that neuronal IFN- γ protects the CNS from tissue damage caused by HTLV-1 infection. Although *IL-12R β 2* is a prime candidate for the gene that controls susceptibility to HAM rat disease, genes involved in the regulation of *IL-12R β 2* are also potential candidates. We envision that IL-12/IL-12 receptor-mediated, neuronal IFN- γ responses are also critically involved in the pathogenesis of human HAM/TSP. Hence, the dissection of the molecular mechanisms leading to the development of HAM rat disease should help us understand the factors that govern susceptibility to human HAM/TSP.

Acknowledgments

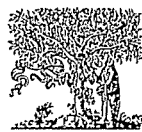
We thank the entire staff of the Institute of Animal Experimentation, Hokkaido University Graduate School of Medicine for their skillful maintenance of rats.

References

1. Poesz BJ, Ruscetti FW, Gazdar AF, Bunn PA, Minna JD, Gallo RC: Detection and isolation of type C retrovirus particles from fresh and cultured lymphocytes of a patient with cutaneous T-cell lymphoma. *Proc Natl Acad Sci USA* 1980, 77:7415-7419
2. Yoshida M, Miyoshi I, Hinuma Y: Isolation and characterization of

- retrovirus from cell lines of human adult T-cell leukemia and its implication in the disease. *Proc Natl Acad Sci USA* 1982, 79:2031-2035
3. Gessain A, Barin F, Vernant JC, Gout O, Maurs L, Calender A, de Thé G: Antibodies to human T-lymphotropic virus type-I in patients with tropical spastic paraparesis. *Lancet* 1985, 2:407-410
 4. Osame M, Usuku K, Izumo S, Ijichi N, Amitani H, Igata A, Matsumoto M, Tara M: HTLV-I associated myelopathy, a new clinical entity. *Lancet* 1986, 1:1031-1032
 5. Mochizuki M, Watanabe T, Yamaguchi K, Takatsuki K, Yoshimura K, Shirao M, Nakashima S, Mori S, Araki S, Miyata N: HTLV-I uveitis: a distinct clinical entity caused by HTLV-I. *Jpn J Cancer Res* 1992, 83:236-239
 6. Nishioka K, Maruyama I, Sato K, Kitajima I, Nakajima Y, Osame M: Chronic inflammatory arthropathy associated with HTLV-I. *Lancet* 1989, 1:441
 7. Sugimoto M, Nakashima H, Watanabe S, Uyama E, Tanaka F, Ando M, Araki S, Kawasaki S: T-lymphocyte alveolitis in HTLV-I-associated myelopathy. *Lancet* 1987, 2:1220
 8. Vernant JC, Buisson G, Magdeleine J, De Thore J, Jouannelle A, Neisson-Vernant C, Monplaisir N: T-lymphocyte alveolitis, tropical spastic paresis, and Sjögren syndrome. *Lancet* 1988, 1:177
 9. Morgan OS, Rodgers-Johnson P, Mora C, Char G: HTLV-1 and polymyositis in Jamaica. *Lancet* 1989, 2:1184-1187
 10. LaGrenade L, Hanchard B, Fletcher V, Cranston B, Blattner W: Infective dermatitis of Jamaican children: a marker for HTLV-I infection. *Lancet* 1990, 336:1345-1347
 11. Hollsberg P, Haller DA: Seminars in medicine of the Beth Israel Hospital, Boston. Pathogenesis of diseases induced by human lymphotropic virus type I infection. *N Engl J Med* 1993, 328:1173-1182
 12. Ishiguro N, Abe M, Seto K, Sakurai H, Ikeda H, Wakisaka A, Togashi T, Tateno M, Yoshiki T: A rat model of human T lymphocyte virus type I (HTLV-I) infection. 1. Humoral antibody response, provirus integration, and HTLV-I-associated myelopathy/tropical spastic paraparesis-like myelopathy in seronegative HTLV-I carrier rats. *J Exp Med* 1992, 176:981-989
 13. Seto K, Abe M, Ohya O, Itakura O, Ishiguro N, Ikeda H, Wakisaka A, Yoshiki T: A rat model of HTLV-I infection: development of chronic progressive myeloneuropathy in seropositive WKAH rats and related apoptosis. *Acta Neuropathol (Berl)* 1995, 89:483-490
 14. Ohya O, Ikeda H, Tomaru U, Yamashita I, Kasai T, Morita K, Wakisaka A, Yoshiki T: Human T-lymphocyte virus type I (HTLV-I)-induced myeloneuropathy in rats: oligodendrocytes undergo apoptosis in the presence of HTLV-I. *APMIS* 2000, 108:459-466
 15. Jacobson S: Immunopathogenesis of human T cell lymphotropic virus type I-associated neurologic disease. *J Infect Dis* 2002, 186(Suppl 2):S187-S192
 16. Kasai T, Ikeda H, Tomaru U, Yamashita I, Ohya O, Morita K, Wakisaka A, Matsuoka E, Moritoyo T, Hashimoto K, Higuchi I, Izumo S, Osame M, Yoshiki T: A rat model of human T lymphocyte virus type I (HTLV-I) infection: in situ detection of HTLV-I provirus DNA in microglia/macrophages in affected spinal cords of rats with HTLV-I-induced chronic progressive myeloneuropathy. *Acta Neuropathol (Berl)* 1999, 97:107-112
 17. Tomaru U, Ikeda H, Ohya O, Abe M, Kasai T, Yamasita I, Morita K, Wakisaka A, Yoshiki T: Human T lymphocyte virus type I-induced myeloneuropathy in rats: implication of local activation of the pX and tumor necrosis factor-alpha genes in pathogenesis. *J Infect Dis* 1996, 174:318-323
 18. Jiang X, Ikeda H, Tomaru U, Morita K, Tanaka Y, Yoshiki T: A rat model for human T lymphocyte virus type I-associated myeloneuropathy. Down-regulation of bcl-2 expression and increase in sensitivity to TNF-alpha of the spinal oligodendrocytes. *J Neuroimmunol* 2000, 106:105-113
 19. Panitch HS, Hirsch RL, Haley AS, Johnson KP: Exacerbations of multiple sclerosis in patients treated with gamma interferon. *Lancet* 1987, 1:893-895
 20. Renno T, Taupin V, Bourbonniere L, Verge G, Tran E, De Simone R, Krakowski M, Rodriguez M, Peterson A, Owens T: Interferon-gamma in progression to chronic demyelination and neurological deficit following acute EAE. *Mol Cell Neurosci* 1998, 12:376-389
 21. Krakowski M, Owens T: Interferon-gamma confers resistance to experimental allergic encephalomyelitis. *Eur J Immunol* 1996, 26:1641-1646
 22. Gao X, Gillig TA, Ye P, D'Ercole AJ, Matsushima GK, Popko B: Interferon-gamma protects against cuprizone-induced demyelination. *Mol Cell Neurosci* 2000, 16:338-349
 23. Finke D, Brinckmann UG, ter Meulen V, Liebert UG: Gamma interferon is a major mediator of antiviral defense in experimental measles virus-induced encephalitis. *J Virol* 1995, 69:5469-5474
 24. Patterson CE, Lawrence DM, Echols LA, Rall GF: Immune-mediated protection from measles virus-induced central nervous system disease is noncytolytic and gamma interferon dependent. *J Virol* 2002, 76:4497-4506
 25. Geiger KD, Nash TC, Sawyer S, Krahl T, Patstone G, Reed JC, Krajewski S, Dalton D, Buchmeier MJ, Sarvetnick N: Interferon-gamma protects against herpes simplex virus type 1-mediated neuronal death. *Virology* 1997, 238:189-197
 26. Miyoshi I, Kubonishi I, Yoshimoto S, Akagi T, Ohtsuki Y, Shiraishi Y, Nagata K, Hinuma Y: Type C virus particles in a cord T-cell line derived by co-cultivating normal human cord leukocytes and human leukaemic T cells. *Nature* 1981, 294:770-771
 27. Bloch G, Toma DP, Robinson GE: Behavioral rhythmicity, age, division of labor and period expression in the honey bee brain. *J Biol Rhythms* 2001, 16:444-456
 28. Peliidou SH, Zou LP, Deretzi G, Nennesmo I, Wei L, Mix E, Van Der Meide PH, Zhu J: Intranasal administration of recombinant mouse interleukin-12 increases inflammation and demyelination in chronic experimental autoimmune neuritis in Lewis rats. *Scand J Immunol* 2000, 51:29-35
 29. Tomaru U, Ikeda H, Jiang X, Ohya O, Yoshiki T: Provirus expansion and deregulation of apoptosis-related genes in the spinal cord of a rat model for human T-lymphocyte virus type I-associated myeloneuropathy. *J Neurovirol* 2003, 9:530-538
 30. Kroger A, Koster M, Schroeder K, Hauser H, Mueller PP: Activities of IRF-1. *J Interferon Cytokine Res* 2002, 22:5-14
 31. D'Onofrio C, Franzese O, Puglianiello A, Peci E, Lanzilli G, Bonmassar E: Antiviral activity of individual versus combined treatments with interferon alpha, beta and gamma on early infection with HTLV-I in vitro. *Int J Immunopharmacol* 1992, 14:1069-1079
 32. Neumann H, Schmidt H, Wilharm E, Behrens L, Wekerle H: Interferon gamma gene expression in sensory neurons: evidence for autocrine gene regulation. *J Exp Med* 1997, 186:2023-2031
 33. Olsson T, Kelic S, Edlund C, Bakhtiet M, Hojeborg B, van der Meide PH, Ljungdahl A, Kristensson K: Neuronal interferon-gamma immunoreactive molecule: bioactivities and purification. *Eur J Immunol* 1994, 24:308-314
 34. Schmidt B, Stoll G, Toyka KV, Hartung HP: Rat astrocytes express interferon-gamma immunoreactivity in normal optic nerve and after nerve transection. *Brain Res* 1990, 515:347-350
 35. Barish ME, Mansdorf NB, Raissdana SS: Gamma-interferon promotes differentiation of cultured cortical and hippocampal neurons. *Dev Biol* 1991, 144:412-423
 36. Vikman K, Robertson B, Grant G, Liljeborg A, Kristensson K: Interferon-gamma receptors are expressed at synapses in the rat superficial dorsal horn and lateral spinal nucleus. *J Neurocytol* 1998, 27:749-759
 37. Frucht DM, Fukao T, Bogdan C, Schindler H, O'Shea JJ, Koyasu S: IFN-gamma production by antigen-presenting cells: mechanisms emerge. *Trends Immunol* 2001, 22:556-560
 38. Watford WT, Moriguchi M, Morinobu A, O'Shea JJ: The biology of IL-12: coordinating innate and adaptive immune responses. *Cytokine Growth Factor Rev* 2003, 14:361-368
 39. van Rietschoten JG, Smits HH, van de Wetering D, Westland R, Verweij CL, den Hartog MT, Wierenga EA: Silencer activity of NFATc2 in the interleukin-12 receptor beta 2 proximal promoter in human T helper cells. *J Biol Chem* 2001, 276:34509-34516
 40. van Rietschoten JG, Westland R, van den Bogaard R, Nieste-Otter MA, van Veen A, Jonkers RE, van der Pouw Kraan TC, den Hartog MT, Wierenga EA: A novel polymorphic GATA site in the human IL-12Rbeta2 promoter region affects transcriptional activity. *Tissue Antigens* 2004, 63:538-546
 41. Rosenzweig SD, Holland SM: Defects in the interferon-gamma and interleukin-12 pathways. *Immunol Rev* 2005, 203:38-47
 42. Watford WT, Hissong BD, Bream JH, Kanno Y, Muul L, O'Shea JJ: Signaling by IL-12 and IL-23 and the immunoregulatory roles of STAT4. *Immunol Rev* 2004, 202:139-156
 43. Xiao BG, Link H: Immune regulation within the central nervous system. *J Neurol Sci* 1998, 157:1-12

44. Eneroth A, Andersson T, Olsson T, Orvell C, Norrby E, Kristensson K: Interferon-gamma-like immunoreactivity in sensory neurons may influence the replication of Sendai and mumps viruses. *J Neurosci Res* 1992, 31:487-493
45. Kohanawa M, Nakane A, Asano M, Minagawa T: Theiler's virus is eliminated by a gamma-interferon-independent mechanism in the brain. *J Neuroimmunol* 1994, 52:79-86
46. Kiefer R, Haas CA, Kreutzberg GW: Gamma interferon-like immunoreactive material in rat neurons: evidence against a close relationship to gamma interferon. *Neuroscience* 1991, 45:551-560
47. Lau LT, Yu AC: Astrocytes produce and release interleukin-1, interleukin-6, tumor necrosis factor alpha and interferon-gamma following traumatic and metabolic injury. *J Neurotrauma* 2001, 18:351-359
48. Xiao BG, Link H: IFN-gamma production of adult rat astrocytes triggered by TNF-alpha. *Neuroreport* 1998, 9:1487-1490
49. Li J, Gran B, Zhang GX, Ventura ES, Siglienti I, Rostami A, Kamoun M: Differential expression and regulation of IL-23 and IL-12 subunits and receptors in adult mouse microglia. *J Neurol Sci* 2003, 215:95-103



ELSEVIER

Available online at www.sciencedirect.com

Experimental and Molecular Pathology xx (2006) xxx–xxx

**Experimental
and Molecular
Pathology**
www.elsevier.com/locate/yexmp

Enhanced production of p24 Gag protein in HIV-1-infected rat cells fused with uninfected human cells

Jing Chen^a, Xudong Zhao^a, Yurong Lai^a, Akira Suzuki^a, Utano Tomaru^a, Akihiro Ishizu^{a,b,*}, Akio Takada^{a,c}, Hitoshi Ikeda^a, Masanori Kasahara^a, Takashi Yoshiki^{a,d}

^a Department of Pathology, Hokkaido University Graduate School of Medicine, Sapporo 060-8638, Japan

^b Department of Health Sciences, Hokkaido University School of Medicine, Sapporo 060-0812, Japan

^c Sapporo City General Hospital, Sapporo 060-8604, Japan

^d Genetic Lab, Sapporo 060-0009, Japan

Received 16 August 2006, and in revised form 25 October 2006

Abstract

Although many human molecules have been suggested to affect replication of human immunodeficiency virus type 1 (HIV-1), the distribution of such cofactors in human cell types is not well understood. Rat W31/D4R4 fibroblasts expressing human CD4 and CXCR4 receptors were infected with HIV-1. The provirus was integrated in the host genome, but only a limited amount of p24 Gag protein was produced in the cells and culture supernatants. Here we found that p24 production was significantly increased by fusing HIV-1-infected W31/D4R4 cells with uninfected human cell lines of T-cell, B-cell, or macrophage lineages. These findings suggest that human cellular factors supporting HIV-1 replication are distributed widely in cells of lymphocyte and macrophage lineages. We also examined whether the amount of p24 produced by rat–human hybrid cells was correlated with expression levels of specific human genes. The results suggested that HP68 and MHC class II transactivator (CIITA) might up- and down-regulate p24 production, respectively. It was also suggested that HIV-1 replication is affected by molecules other than those examined in this study, namely, cyclin T1, cyclin-dependent kinase 9, CRM1, HP68, and CIITA.

© 2006 Elsevier Inc. All rights reserved.

Keywords: HIV-1; Rat model; Cell fusion; Cyclin T1; CDK9; CRM1; HP68; CIITA

Introduction

Replication of human immunodeficiency virus type 1 (HIV-1) is initiated by binding of the viral envelope to the specific surface receptors on target cells. The viral envelope gp120 glycoprotein binds to a human CD4 molecule expressed on T cells and macrophages. A chemokine receptor CXCR4 on T cells or CCR5 on macrophages is also required for virus entry into cells (Kozak et al., 1997). CD4 molecules and chemokine receptors of rodents, which are naturally resistant to HIV-1 infection, do not bind to gp120; therefore, a major barrier to HIV-infection exists at the level of virus entry

(Pleskoff et al., 1997). Recent studies showed that rat-derived cells expressing human CD4 and CXCR4 or CD4 and CCR5 became susceptible to HIV-1 viruses (Keppler et al., 2001). However, the rat cell lines produced infectious virus particles still at much lower levels than in human cells, suggesting the existence of additional human factors important for HIV-1 replication.

Over the past couple of decades, several critical steps in HIV-1 replication have been identified. HIV-1 gene expression relies upon complex machinery controlled by two viral regulatory proteins, Tat and Rev. Tat activates the transcription of the viral genome and requires the cellular protein kinase activity termed TAK/P-TEFb, composed of cyclin T1 and cyclin-dependent kinase 9 (CDK9), for its transactivation function (Herrmann and Rice, 1995; Chen et al., 1999). It is reported that the host MHC class II transactivator (CIITA) is recruited instead of Tat during an early phase of

* Corresponding author: Department of Health Sciences, Hokkaido University School of Medicine, Kita-12, Nishi-5, Kita-ku, Sapporo 060-0812, Japan. Fax: +81 11 706 4916.

E-mail address: aishizu@med.hokudai.ac.jp (A. Ishizu).

infection (Saifuddin et al., 2000). Rev is necessary for the accumulation of incompletely spliced HIV-1 RNAs in the nucleus and exports them to the cytoplasm cooperating with the cellular exportin 1/CRM1 molecule (Cmarko et al., 2002). During HIV-1 assembly, Gag polypeptides multimerize into immature HIV-1 capsids. The cellular ATP-binding protein, HP68, is required for this process (Zimmerman et al., 2002; Lingappa et al., 2006).

Although many human molecules have been suggested to affect HIV-1 infection and replication, the distribution of such cofactors in human cell types is not well understood. Here we infected rat fibroblasts coexpressing human CD4 and CXCR4 with HIV-1, fused them with uninfected human cell lines of T-cell, B-cell, or macrophage lineages, and then examined virus production and expression profiles of human genes in the fused cells.

Materials and methods

Cells

Rat W31 fibroblasts (Kanki et al., 2000) were transfected with plasmids carrying the human CD4 gene and those carrying the CXCR4 gene. The expression plasmid of the human CD4 gene (Yamamura et al., 1991) was kindly provided by Dr. Karasuyama (Tokyo Medical and Dental University, Tokyo, Japan). The CXCR4 cDNA was amplified using total RNAs extracted from human peripheral blood mononuclear cells and then subcloned into the pcDNA3.1/Zeo vector (Invitrogen, Carlsbad, CA). Transfection was carried out using Lipofectamine (Invitrogen) according to the manufacturer's protocol. The transfectant, designated as W31/D4R4 cells, was maintained in DMEM supplemented with 10% fetal calf serum (FCS), 400 µg/ml of G418 (GIBCO-BRL, Rockville, MD), and 40 µg/ml of Zeocine (Invitrogen). Several weeks later, cloned W31/D4R4 cells were obtained with limiting dilution.

Human cell lines, including Hut78 and Jurkat (T-cell lymphoma), U937 (macrophage-like cell line), and GI, Raji, Swei, and WT46 (B-cell lymphoma), were cultured in RPMI 1640 medium supplemented with 10% FCS.

HIV-1 infection

W31/D4R4 cells (5×10^5) were pretreated with 2 µg/ml of polybrene for 30 min and then the T-tropic HIV-1 strain, SF33 (Tateno and Levy, 1988), was applied to the cells (equivalent to 200 ng of p24 Gag protein) followed by incubation for 3 h at 37 °C. The supernatants were then removed, and cells were washed 3 times with PBS and digested by trypsin to remove viruses that had not entered the cells. The cells were resuspended in the selection medium and cultured at 37 °C.

PCR and RT-PCR for HIV-1 genes

Genomic DNAs were extracted from the HIV-1-infected W31/D4R4 cells by the standard method. Total RNAs were extracted from the cells with TRIzol Reagent (Invitrogen). The RNAs were subjected to DNase I treatment to remove contaminating DNAs. cDNAs were synthesized with 4 µg of the DNase-treated RNAs using the SuperScript III kit (Invitrogen). PCR for HIV-1 genes was performed using primer sets described previously (York-Higgins et al., 1990; Brandt et al., 1992).

ELISA for p24 Gag protein

HIV-1 p24 Gag protein was quantified using the p24 assay ELISA kit (Zeptomatrix, Buffalo, NY). Culture supernatants and cell lysates were

subjected to this assay. Tissue culture medium was changed with a fresh one 24 h prior to the assay. The supernatants were centrifuged to remove cell debris; 450 µl of the solution was taken and then mixed with 50 µl of the lysis buffer appended to the kit. The resultant mixture served as culture supernatant samples. For cell lysate samples, 1×10^7 cells were resuspended in 450 µl of fresh medium and then mixed well with 50 µl of the lysis buffer. After centrifugation for removal of the pellets, the supernatants were used as cell lysate samples.

Cell fusion

HIV-1-infected W31/D4R4 cells were maintained for 3 months. Cells (5×10^6) were then washed extensively with PBS, digested by trypsin, and mixed with an equal number of human cells. The mixed cell pellets were overlaid with 1 ml of a 50% solution of polyethylene glycol and stirred gently. After incubation at 37 °C for 1 min, PBS was added slowly followed by centrifugation ($500 \times g$ for 5 min) to remove supernatants. The pellets were resuspended in the selection medium and incubated at 37 °C. The medium was changed with a fresh one every 3 or 4 days. Three weeks later, p24 concentrations were determined in the fused cells and culture supernatants, and the expression of human genes in the rat–human hybrid cells was examined by RT-PCR (see RT-PCR for human genes).

To evaluate the efficiency of cell fusion, human cells were labeled with PKH26 Red Fluorescent Cell Linker Kit (Sigma-Aldrich, St. Louis, MO), according to the manufacturer's protocol, prior to cell fusion. The labeled cells were then fused with uninfected W31/D4R4 cells as described above. Fused cells were incubated in the selection medium at 37 °C for 1 week. The percentage of fused cells was calculated by dividing the number of fluorescence-labeled cells by that of living cells.

RT-PCR for human genes

Expression of human genes, including cyclin T1, CDK9, CRM1, HP68, and CIITA, was examined by RT-PCR. Hybrid cells were harvested 21 days after fusion, and total RNAs were extracted and then subjected to cDNA synthesis. cDNAs were also prepared from parental human cells that were not subjected to fusion with W31/D4R4 cells. The first round of PCR was run for 15 cycles (95 °C for 30 s, annealing for 30 s, 72 °C for 30 s) with sense 1 and antisense 1 primers. The second round of PCR was run for 35 cycles (95 °C for 30 s, annealing for 30 s, 72 °C for 30 s) with sense 2 and antisense 2 primers. Primer sequences and the annealing temperature are shown in Table 1. These primer sets were specific for the human genes and did not amplify the corresponding rat genes.

Table 1
Primers used for RT-PCR

Name of genes		Sequences (5' to 3')	Annealing temperature
Cyclin T1	Sense 1 (2) ^a	agctggaaaatagcccatcc	60 °C
	Antisense 1	aggagggttctgatggcagag	
	Antisense 2	ctgctggagccacagaattt	
CDK9	Sense 1	gccaagatcggccaaggcaccctcgg	56 °C
	Sense 2	ggtgttcaaggccaggcaccgca	
	Antisense 1 (2) ^a	cccatcacgagtgataagcaccatla	
CRM1	Sense 1	tgltggagcaantagggaccag	55 °C
	Sense 2	gcaatgcatgaaggagacga	
	Antisense 1 (2) ^a	cctgaacctgaacgaaatgc	
HP68	Sense 1	gagttgctctgtagttcgaatc	55 °C
	Sense 2	gtacgatgatcctctgactggc	
	Antisense 1	aacttccctcctgaagatcttca	
CIITA	Antisense 2	tcgttcttttagtgggtaaatca	60 °C
	Sense 1 (2) ^a	ctgggattcctacacaatgcg	
	Antisense 1	ctgggatcatctcaggctga	
	Antisense 2	tcagcatcgtgtaagaagctc	

^a The same primer was used for the first and second rounds of PCR.

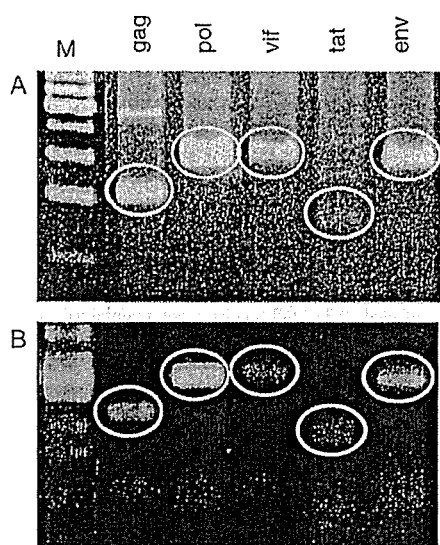


Fig. 1. Integration of the provirus (A) and expression of viral mRNAs (B). W31/D4R4 cells were infected with HIV-1. Genomic DNAs and total RNAs were extracted from the cells 3 months after infection, and then integration of the provirus and expression of viral mRNAs were examined by PCR and RT-PCR, respectively. Ovals indicate specific PCR products. Product size: *gag*, 213 bp; *pol*, 307 bp; *vif*, 321 bp; *tat*, 159 bp; and *env*, 321 bp. M, 100-bp ladder marker.

Statistics

Data were analyzed with Student's *t*-test. *P*-values less than 0.05 were considered to be significant.

Results

Integration and expression of viral genes in W31/D4R4 cells infected with HIV-1

W31/D4R4 cells were infected with the T-tropic HIV-1 strain, SF33. Three months later, genomic DNAs and total RNAs were extracted from the HIV-1-infected cells, and then integration of provirus and expression of viral mRNAs were examined by PCR and RT-PCR, respectively.

Integration of HIV-1 provirus was confirmed by PCR with 5 pairs of primers, each specific for the *gag*, *pol*, *vif*, *tat*, or *env* region of the HIV-1 genome (Fig. 1A). Expression of viral mRNAs, including *gag*, *pol*, *vif*, *tat*, and *env*, was detected by RT-PCR (Fig. 1B). By contrast, RNAs without reverse transcription did not generate visible PCR products, indicating minimal contamination of genomic DNAs in the RNA sample (data not shown). These findings suggested that W31/D4R4 cells were infected with HIV-1 and that integration of provirus was accomplished and viral mRNAs were expressed in the rat cells.

Production of p24 Gag protein in W31/D4R4 cells infected with HIV-1

We examined the production of viral proteins in HIV-1-infected W31/D4R4 cells by measuring p24 Gag concentrations

in the cell lysates and culture supernatants. Samples were collected at days 2, 4, 7, 14, 21, and 28 post-infection, and the amount of HIV-1 Gag protein was measured using the p24 ELISA kit. p24 in the cell lysates showed a peak concentration of >10,000 pg/ml at day 4 post-infection and decreased to 84 pg/ml at day 28 post-infection (Fig. 2). Even 3 months later, p24 in the cell lysates retained a concentration of 12 pg/ml (data not shown). On the other hand, p24 in the supernatants showed a peak concentration of >1000 pg/ml at day 4 post-infection, but decreased rapidly, and fell below the detection limit at day 28 post-infection.

Production of p24 Gag protein in fused cells

Three months after HIV-1 infection, the infected W31/D4R4 cells were fused with human cell lines. Cell lysates and culture supernatants were subjected to ELISA at day 21 after cell fusion. p24 concentration in the cell lysates showed a 4- to 10-fold increase when the HIV-1-infected W31/D4R4 cells were fused with an uninfected human T-cell lymphoma line Hut 78, a macrophage-like cell line U937, and B-cell lymphoma lines GI, Swei, and WT 46 (Fig. 3A). Although there was no statistically significant difference, fusion with the B-cell lymphoma line Raji also increased the concentration of p24 in the cell lysates. On the other hand, no significant increase was seen when HIV-1-infected W31/D4R4 cells were fused with the human T-cell lymphoma line Jurkat.

Fusion with human cells generally failed to increase p24 concentration in the culture supernatants (Fig. 3B). However, p24 concentration showed a slight but statistically significant increase (10 pg/ml) when the HIV-1-infected W31/D4R4 cells were fused with the B-cell lymphoma line WT46.

Alteration of human gene expression after cell fusion

Expression of human cyclin T1, CDK9, CRM1, HP68, and CIITA genes was examined by RT-PCR in both parental

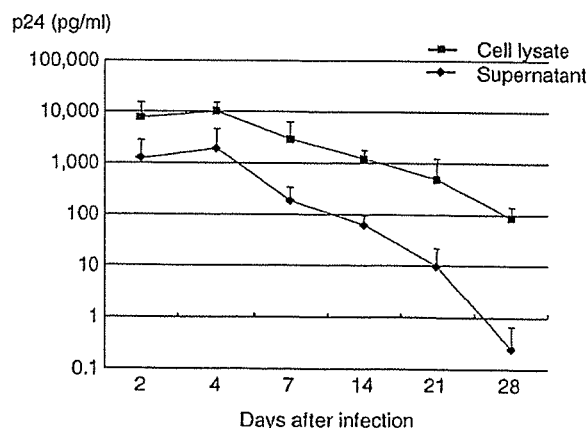


Fig. 2. Production of p24 in HIV-1-infected W31/D4R4 cells. W31/D4R4 cells were infected with HIV-1. Cell lysates and culture supernatants were collected at days 2, 4, 7, 14, 21, and 28 post-infection, and the amount of HIV-1 p24 Gag protein was measured using the ELISA kit.

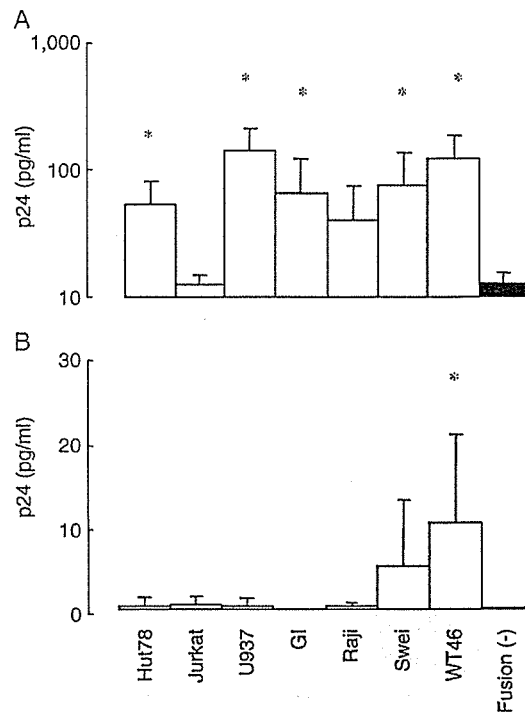


Fig. 3. Production of p24 in HIV-1-infected W31/D4R4 cells fused with uninfected human cells. HIV-1-infected W31/D4R4 cells were fused with indicated human cells. Cell lysates (A) and culture supernatants (B) were subjected to ELISA at day 21 after fusion (* $p < 0.05$).

human cell lines and rat–human hybrid cells. For this analysis, we used the same batch of hybrid cells as used in Fig. 3. Cyclin T1, CDK9, CRM1, and HP68 genes were expressed in all the human cell lines examined (Fig. 4, left panels). Notably, expression of CIITA was not detected in Jurkat (see asterisk).

After cell fusion, expression of human genes was largely extinguished (Fig. 4, right panels). None of the hybrid cells expressed human CDK9 or CRM1. Expression of cyclin T1 was seen exclusively in W31/D4R4 cells fused with Raji, and HP68 was expressed only in W31/D4R4 cells fused with WT46. The human CIITA gene, expressed in Hut78, U937, and the B-cell lymphoma lines, lost its expression after fusion. On the contrary, expression of CIITA was induced in W31/D4R4–Jurkat hybrid cells.

Discussion

Development of a small animal model of HIV-1 infection would greatly facilitate studies of virus transmission, pathogenesis, host immune responses, and antiviral strategies. Mice and rats are attractive models for HIV-1 study because they can be genetically manipulated. However, the development of a permissive model has been hampered by the inability of HIV-1 to infect primary rodent cells.

Rodent CD4 and CXCR4/CCR5 (receptors for HIV-1) do not bind to the viral envelope gp120 (Pleskoff et al., 1997). Transgenic mouse and rat cells, expressing human CD4 and

CXCR4 or CD4 and CCR5, became susceptible to HIV-1 infection, and the provirus could be integrated in the host genome (Sawada et al., 1998; Keppler et al., 2001). However, replication of the infectious virus remained at much lower levels in these rodent cells than in human cells, thus suggesting the involvement of additional human genes in virus replication (Freed, 2004; Trkola, 2004). Indeed, it has been reported that human but not rodent cyclin T1 supports the function of viral Tat protein (Keppler et al., 2001). One of the effective ways to identify human molecules contributing to HIV-1 replication is to conduct cell fusion experiments using human and rodent cells. Identification of such molecules and subsequent introduction into rodents should help us establish animal models of HIV-1 infection.

Although several human molecules have been suggested to affect HIV-1 replication, the distribution of such cofactors in human cell types is not well understood. In the present study, rat fibroblasts transgenic for human CD4 and CXCR4 genes, W31/D4R4, were infected with HIV-1. These cells were fused with uninfected human cell lines of T-cell, B-cell, or macrophage origin followed by the assessment of associations between viral production and human gene expression.

As expected, rat W31/D4R4 cells could be infected with HIV-1, and the provirus was integrated in the host genome (Fig. 1A). Expression of virus genes was detectable by RT-PCR even 3 months after infection (Fig. 1B), but the concentration of p24 Gag protein was very low in the cell lysates (12 pg/ml) and was below the detection limit in the culture supernatants (Fig. 2). Poor production of p24 may have occurred because rat cells infected with HIV-1 died or were unable to proliferate like their uninfected counterparts and/or because host factors supporting viral replication were deficient in rat cells. Since we observed no significant difference in the viability and proliferation of W31/D4R4 cells before and after HIV-1 infection, the first possibility appeared unlikely. Thus, we conducted cell fusion experiments using HIV-1-infected W31/D4R4 cells and uninfected human cell lines.

We found significant recovery of the expression of p24 Gag protein in the HIV-1-infected W31/D4R4 cells upon fusion with the human T-cell lymphoma line Hut78, macrophage-like cell line U937, and B-cell lymphoma lines GI, Swei, and WT46 (Fig. 3A). These findings indicate that human factors that support HIV-1 replication are distributed widely in cells of lymphocyte and macrophage lineages.

To examine whether the amount of p24 produced by hybrid cells is correlated with expression levels of specific human genes, we analyzed expression of cyclin T1, CDK9, CRM1, HP68, and CIITA genes in the fused cells. We chose these genes for study because they have been suggested to affect HIV-1 replication (Herrmann and Rice, 1995; Chen et al., 1999; Saifuddin et al., 2000; Cmarko et al., 2002; Zimmerman et al., 2002; Lingappa et al., 2006). As shown in Fig. 4, expression of most human genes was lost or down-regulated after cell fusion. By contrast, expression of rat genes coding for cyclin T1, CDK9, CRM1, HP68, and CIITA was not altered (data not shown). These observations indicate that human genes are preferentially lost or inactivated by cell fusion. Some hybrid